Int. J. Heat Mass Transfer. Vol. 5, pp. 373–407. Pergamon Press 1962. Printed in Great Britain.

MASS TRANSFER THROUGH LAMINAR BOUNDARY LAYERS—8. FURTHER SOLUTIONS TO THE VELOCITY EQUATION

H. L. EVANS

Commonwealth Scientific and Industrial Research Organization,
Division of Food Preservation, P.O. Box 43, Ryde, N.S.W., Australia

(*Received* 13 *June* 1961)

Abstract—The paper is concerned with the velocity boundary layer when the fluid properties are uniform and mass is transferred in either direction through the wall boundary. The "similar" form of the velocity equation is used to examine the asymptotic behaviour of boundary-layer functions for large mass-transfer rates. The values of the thickness ratios H_{14}, H_{12} and H_{24} for intensive blowing are tabulated.

The method used for integrating the equation on a computer is described, and the following numerical solutions are given. (1) Accurate solutions for $\beta = 1$, the forward stagnation point for two-dimensional flow, the mass-transfer parameter f_0 being given the thirteen values $-3{\cdot}0$ (0·5) 3·0. (2) Accurate solutions for $\beta = -1$ in the real domain; the mass-transfer parameter f_0 takes eight values from $\sqrt{2}$ at the separation point to $\sqrt{10}$, which is approaching asymptotic suction. (3) Solutions of slightly lower accuracy in the real domain for zero mass transfer when β has large values. (4) Interpolated solutions when β is infinite, which include the effect of mass transfer; for this set both real and imaginary values of the variables are included.

Curves are drawn showing the variation with pressure gradient of the rate-of-growth function F_2 and the thickness ratio H_{24} for mass-transfer rates in the range $0 \leqslant (v_0\,\delta_2/\nu) \leqslant 20{\cdot}0$. In an Appendix, formulae are given for evaluating high-order derivatives of the stream function.

NOMENCLATURE

Where the quantities in the following list have dimensions these are given in brackets after the definitions; otherwise they are dimensionless. The symbols used in Appendices B and C are not included.

C, constant occurring in equation (7);

E_2, a correction to the linear approximation for the relationship between F_2 and λ_2 when mass transfer is zero, defined by equation (101);

F_2, function giving the rate of growth of the momentum thickness with distance x, defined in equation (44);

f, dimensionless stream function defined by equation (17);

f_0, value of f at the wall boundary; a measure of the rate at which mass flows through the wall and related to the velocity v_0 by equation (20);

f_0'', second derivative of f with respect to η evaluated at the wall boundary; a measure of the shear stress at the wall;

$\bar{f}$, the real form of f in the imaginary domain, defined in equation (21);

$\bar{f}_0$, the real form of f_0 in the imaginary domain, related to the velocity v_0 by equation (24);

H_{12}, ratio of displacement to momentum boundary-layer thickness; for similar solutions defined by equation (40);

H_{14}, ratio of displacement to shear boundary-layer thickness; for similar solutions it is δ_1^*/δ_4^*;

H_{24}, ratio of momentum to shear boundary-layer thickness; for similar solutions defined by equation (41);

k_0, mass-transfer parameter for the case when β is infinite (see Section 2.3); related to the velocity v_0 by equation (26);

$\bar{k}_0$, the real form of k_0 in the imaginary domain, related to the velocity v_0 by equation (33);
L, value of $(1 - \theta')/\theta''$ in the main-stream, related to the parameter k_0 by equation (106);
L_1, value of $(1 - \bar{\theta}')/\bar{\theta}''$ in the main-stream, related to the parameter $\bar{k}_0$ by equation (108);
n, constant occurring in equation (7);
u, velocity component parallel to the wall (ft/h);
u_G, value of u in the main-stream (ft/h);
v, velocity component perpendicular to the wall (ft/h);
v_0, value of v at the wall (ft/h);
x, distance parallel to the wall measured from the start of the boundary layer (ft);
y, distance perpendicular to the wall measured from the wall towards the main-stream (ft).

Greek symbols

β, parameter occurring in the similar form of the velocity equation; defined by equation (15);
δ_1, displacement boundary-layer thickness $= \int_0^\infty (1 - u/u_G)\,dy$, (ft);
δ_1^*, displacement boundary-layer thickness in terms of the appropriate similar length co-ordinate; when the latter is η it is defined by equation (34);
δ_2, momentum boundary-layer thickness $= \int_0^\infty (u/u_G)(1 - u/u_G)\,dy$, (ft);
δ_2^*, momentum boundary-layer thickness in terms of the appropriate similar length co-ordinate; when the latter is η it is defined by equation (35);
δ_4, shear boundary-layer thickness $= u_G/(\partial u/\partial y)_{y=0}$, (ft);
δ_4^*, shear boundary-layer thickness in similar co-ordinates; an alternative expression for $1/f_0''$;
ζ, dimensionless stream function defined by equation (9);
ζ_0, value of ζ at the wall boundary; a measure of the rate at which mass flows through the wall and related to the velocity v_0 by equation (14);
η, dimensionless similar length co-ordinate defined by equation (16);
$\bar{\eta}$, real form of η in the imaginary domain; defined in equation (21);
θ, stream function for the case of infinite β for real values of the variables, defined as $(\zeta - \zeta_0)$;
$\bar{\theta}$, real form of θ when the variables are pure imaginary, defined in equation (29);
λ_2, pressure-gradient parameter relating to the momentum thickness; defined in equation (43);
ν, kinematic viscosity of fluid (ft²/h);
ξ, dimensionless similar length co-ordinate, defined by equation (8);
$\bar{\xi}$, real form of ξ when the variables are pure imaginary, defined in equation (29);
q, dimensionless stream function for intensive blowing, defined by equation (60);
q_0, value of q at the wall boundary;
q_1, dimensionless stream function for intensive suction, defined by equation (46);
q_2, dimensionless stream function for intensive blowing for the case when β is infinite, defined by equation (81);
χ, dimensionless similar length co-ordinate for intensive blowing, defined by equation (59);
χ_1, dimensionless similar length co-ordinate for intensive suction, defined by equation (45);
χ_2, dimensionless similar length co-ordinate for intensive blowing for the case when β is infinite, defined by equation (80);
ψ, stream function defined by equation (4) (ft²/h).

1. INTRODUCTION

1.1 *Earlier Work*

THE first two papers in the present series considered the velocity equation of the laminar boundary layer when mass flows in either direction through the wall boundary. Paper 1, Spalding [1], presented a method of estimating boundary-layer thicknesses and the shear stress at the wall for any two-dimensional, laminar boundary layer for which the fluid properties are uniform, provided the distributions along the wall of the following two quantities are specified:

(i) the pressure gradient in the main-stream, and
(ii) the rate at which mass flows through the wall.

In order to apply this method, "similar" solutions to the boundary-layer equations are required in the form of numerical tables. For application to practical problems, these solutions must cover wide ranges in the parameters specifying the two quantities mentioned above.

All such solutions which could be found in the literature were tabulated in Paper 2, Spalding and Evans [2], where it was shown that "similar" solutions exist both for real and for pure imaginary values of the variables.

Although many solutions were available, they were fairly widely scattered, most of them occurring in that part of the real domain relating to accelerated main-streams. Enough solutions were found in this region to cover much of it by interpolation between the exact points. By interpolating for ratios of boundary-layer thicknesses, which in this region vary comparatively slowly with mass-transfer rate, the accuracy was expected to be better than $\pm 0{\cdot}3$ per cent of the values given.

Work done since Paper 2 was written has shown that the accuracy of the interpolated solutions for no mass transfer and for suction is as good as this estimate. The solutions for blowing, on the other hand, are less accurate, the greatest error in the thickness ratios probably approaching ± 1 per cent of the values given. The interpolation procedures involved the use of the asymptotic values of thickness ratios for intensive blowing, and a large part of the error in the interpolated solutions is now thought to be due to inaccuracy in these asymptotic values. The latter are given to high accuracy in Table 1 of the present paper.

Wide areas which are of practical interest were, however, very sparsely covered in the literature. Except for a series of exact points for the case of no mass transfer and a few points of low accuracy for slight deceleration with mass transfer, the region of decelerated main-streams contained very few solutions. The imaginary domain had received even less attention, since only two solutions, both on the line for no mass transfer, were known in that region.

Paper 7, Evans [3], contained some solutions for the case of no mass transfer in the real domain which were more accurate than those given in earlier papers.

1.2 *Outline of Present Paper*

The present paper is concerned exclusively with the velocity boundary layer and reports advances which have been made since the earlier papers in the series were written. In particular, a number of similar solutions are given, most of which are new. These are indicated diagrammatically on the F_2–λ_2 plane in Fig. 1.

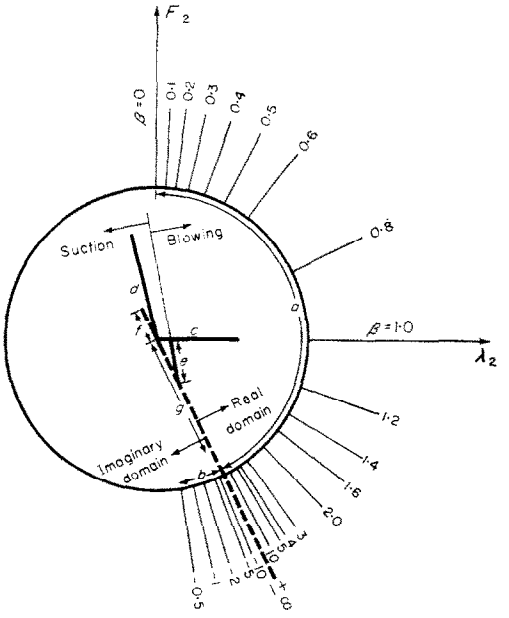

FIG. 1. Illustrating diagrammatically on the F_2–λ_2 plane the solutions given in the present paper. *a*—asymptotic blowing in the real domain (Section 4); *b*—asymptotic blowing in the imaginary domain (Section 4); *c*—two-dimensional forward stagnation point, $\beta = 1$ (Section 6); *d*—$\beta = -1$ in the real domain (Section 7); *e*—high values of β for $f_0 = 0$ in the real domain (Section 8); *f*—interpolated solutions for infinite β when variables are pure imaginary (Section 9); *g*—interpolated solutions for infinite β when variables are real (Section 9).

In section 2 the forms of the similar velocity equation for real and pure imaginary values of the variables are given, and section 3 contains

relationships which are used to evaluate functions required in the present work from tables of numerical solutions.

Section 4 is concerned with the asymptotic behaviour of the boundary layer when the rate of mass transfer through the wall boundary becomes very large. The case of inward mass transfer is only briefly discussed, as this has already received detailed treatment in the literature. The case of outward mass transfer is considered in greater detail.

After the asymptotic form of the differential equation is derived, formulae are obtained for the asymptotic values of f_0'' and the thickness ratios H_{14}, H_{12} and H_{24}. A table of these ratios is then given for suitable values of the parameter β in both the real and the imaginary domains. These asymptotic solutions are indicated in Fig. 1 by the radiating lines outside the unit circle; some values of β have been omitted for clarity. The real domain is indicated by *a* and the imaginary domain by *b*.

The velocity equation is extremely difficult to integrate for high rates of outward mass transfer. It should, however, be easier to integrate the transformed equation given in section 4, either by the usual numerical methods or by obtaining asymptotic expansions in inverse powers of the mass-transfer parameter f_0.

The method used for obtaining numerical solutions with a computer is described in section 5 and Appendix B.

Solutions for the two-dimensional forward stagnation point with mass transfer are given in section 6. Most of these are new and are, in general, more accurate than the solutions for this case quoted in Paper 2. These solutions occur along the line *c* in Fig. 1.

When $\beta = -1$, it was found that the wall shear f_0'' is a simple function of the mass-transfer parameter f_0. This meant that solutions could be obtained on a computer with relative ease. Solutions in the real domain are given in section 7 and occur along the line *d* in Fig. 1; the imaginary domain for this value of β is not considered in the present paper.

Section 8 contains solutions in the real domain for zero mass transfer and high values of the parameter β. These occur along the line *e* in Fig. 1.

The two cases when β is infinite are considered in section 9. Interpolated solutions are given which cover a wider range of mass-transfer rate than those contained in Paper 2. As the solutions are not to high accuracy, they are represented by a broken line in Fig. 1, the portion *g* of this line indicating the solution for real values of the variables and the portion *f* that when the variables are pure imaginary.

2. FORMS OF THE VELOCITY EQUATION IN SIMILAR CO-ORDINATES

2.1 *Transforming the Co-ordinates*

Later parts of the present paper will contain some discussion of the behaviour of the velocity boundary layer, and in many places in this discussion it will be necessary to refer to equations and quantities which occur in the transformation of the boundary-layer equations to similar co-ordinates. The transformation, in the form first given by Spalding [1], is therefore given below. For further discussion of the general behaviour of boundary-layer functions and the roles played by various parameters, the reader is referred to earlier papers in the series, particularly Papers 1 and 2.

For two-dimensional, laminar flow with uniform fluid properties, the equation of motion for fluid in the boundary layer is:

$$u\frac{\partial u}{\partial x} + v\frac{\partial u}{\partial y} = u_G\frac{\mathrm{d}u_G}{\mathrm{d}x} + \nu\frac{\partial^2 u}{\partial y^2} \qquad (1)$$

and the continuity equation is:

$$\frac{\partial u}{\partial x} + \frac{\partial v}{\partial y} = 0. \qquad (2)$$

In these equations:

x = distance measured parallel to the wall,
y = distance measured perpendicular to the wall towards the main-stream,
u = velocity component in the x-direction,
u_G = value of u in the main-stream,
v = velocity component in the y-direction, and
ν = kinematic viscosity of the fluid.

When mass flows through the wall with velocity v_0, the boundary conditions associated with equations (1) and (2) are:

$$\left.\begin{aligned} &y = 0, \quad u = 0, \quad v = v_0 \\ &y \to \infty, \quad u \to u_G. \end{aligned}\right\} \quad (3)$$

The value of v_0 is positive when in the positive y-direction.

Equations (1) and (2) are combined by introducing the stream function ψ defined by:

$$u = \frac{\partial \psi}{\partial y}, \quad v = -\frac{\partial \psi}{\partial x}, \quad (4)$$

so that equation (2) is automatically satisfied and equation (1) becomes:

$$\frac{\partial \psi}{\partial y}\frac{\partial^2 \psi}{\partial x \partial y} - \frac{\partial \psi}{\partial x}\frac{\partial^2 \psi}{\partial y^2} = u_G \frac{du_G}{dx} + \nu \frac{\partial^3 \psi}{\partial y^3} \quad (5)$$

and the boundary conditions from equation (3) are:

$$\left.\begin{aligned} &y = 0, \quad \frac{\partial \psi}{\partial y} = 0, \quad \frac{\partial \psi}{\partial x} = -v_0 \\ &y \to \infty, \quad \frac{\partial \psi}{\partial y} \to u_G. \end{aligned}\right\} \quad (6)$$

Solution of equation (5) with boundary conditions (6) for a general distribution with x of the functions u_G and v_0 is rarely attempted. For certain physical configurations known as "similar" systems, however, these distributions are such that the equation reduces to an ordinary differential equation which, although only rarely soluble analytically, may be integrated accurately by numerical methods.

It was shown in Paper 1 that equation (5) possesses similar solutions when the mainstream velocity obeys the relation:

$$\frac{du_G}{dx} = C u_G^n \quad (7)$$

where C and n are constants.

If the independent length co-ordinate is taken as:

$$\xi = y\left(\frac{1}{\nu}\frac{du_G}{dx}\right)^{1/2} \quad (8)$$

and the new stream function ζ, which is a function of ξ alone, is related to ψ by:

$$\zeta = \frac{\psi}{u_G}\left(\frac{1}{\nu}\frac{du_G}{dx}\right)^{1/2}, \quad (9)$$

the velocity components take the form:

$$u = u_G\left(\frac{d\zeta}{d\xi}\right) \quad (10)$$

$$v = -\left(\nu \frac{du_G}{dx}\right)^{1/2}\left\{\frac{n}{2}\xi\frac{d\zeta}{d\xi} + \left(1 - \frac{n}{2}\right)\zeta\right\}. \quad (11)$$

Using the transformation defined by equations (8) and (9), equation (5) then becomes:

$$\zeta''' + (1 - n/2)\zeta\zeta'' + (1 - \zeta'^2) = 0 \quad (12)$$

with boundary conditions:

$$\left.\begin{aligned} &\xi = 0, \quad \zeta = \zeta_0, \quad \zeta' = 0 \\ &\xi \to \infty, \quad \zeta' \to 1. \end{aligned}\right\} \quad (13)$$

The primes in equations (12) and (13) denote differentiation with respect to ξ.

For similar solutions, the quantity ζ_0 occurring in equation (13) is a constant. From equation (11) this is related to the velocity v_0, at which mass flows through the wall boundary, by:

$$\zeta_0 = \frac{-v_0}{[1 - (n/2)]\{\nu (du_G/dx)\}^{1/2}} \quad (14)$$

so that v_0 varies along the wall as $x^{n/2}$.

Equation (12), with boundary conditions (13), represents one form of the velocity equation in similar co-ordinates. This will be referred to later. The form generally found in the literature and used in the preceding papers of the present series is obtained by using a slightly different transformation from that specified by equations (8) and (9).

If the parameter n is replaced by the parameter β, defined by:

$$\beta = \frac{1}{[1 - (n/2)]}, \quad (15)$$

and the transformation:

$$\eta = y\left(\frac{1}{\nu\beta}\frac{du_G}{dx}\right)^{1/2} \quad (16)$$

$$f = \frac{\psi}{u_G}\left(\frac{1}{\nu\beta}\frac{du_G}{dx}\right)^{1/2} \quad (17)$$

is used, equation (5) then takes the familiar form:

$$\boxed{f''' + ff'' + \beta(1 - f'^2) = 0} \quad (18)$$

with boundary conditions:

$$\left.\begin{aligned} &\eta = 0, \quad f = f_0, \quad f' = 0 \\ &\eta \to \infty, \quad f' \to 1, \end{aligned}\right\} \quad (19)$$

where the primes in equations (18) and (19) denote differentiation with respect to η.

Although boundary conditions (19) are sufficient to define the mathematical problem, other supplementary conditions are often useful and sometimes necessary in order to obtain unique solutions. Two such conditions are:

$$\left.\begin{aligned} &0 \leqslant f' \leqslant 1 \text{ everywhere, and} \\ &f' \to 1 \quad \text{exponentially as } \eta \to \infty. \end{aligned}\right\} \quad (19a)$$

The first of these ensures that the solutions conform with real boundary layers, since it excludes solutions involving reversal of flow (i.e. negative f') as well as those involving velocities in the boundary layer exceeding that in the main-stream (i.e. $f' > 1$). All the solutions considered in the present series of papers satisfy this condition.

The second of the supplementary conditions (19a), which specifies a sufficiently rapid approach to main-stream flow, is sometimes required in order to ensure that the solution is unique.

For the form of the velocity equation given in equation (18), the relationship corresponding to equation (14) is:

$$f_0 = \frac{-v_0}{\sqrt{[(\nu/\beta)(\mathrm{d}u_G/\mathrm{d}x)]}}. \quad (20)$$

Most of the following discussion of laminar boundary layers with mass transfer will refer to equation (18) with boundary conditions (19).

2.2 *The Form of the Equation in the Imaginary Domain*

When the parameter β and the main-stream velocity gradient $\mathrm{d}u_G/\mathrm{d}x$ have opposite signs in the transformation defined by equations (16) and (17), both η and f are pure imaginary. To obtain the differential equation and boundary conditions for this imaginary domain, new real variables $\bar{\eta}$ and $\bar{f}$ are defined by:

$$\left.\begin{aligned} \eta &= i\bar{\eta} \\ f &= i\bar{f}. \end{aligned}\right\} \quad (21)$$

Inserting these into equation (18) gives:

$$-\bar{f}''' + \bar{f}\bar{f}'' + \beta(1 - \bar{f}'^2) = 0 \quad (22)$$

and the boundary conditions (19) become:

$$\left.\begin{aligned} &\bar{\eta} = 0, \quad \bar{f} = \bar{f}_0, \quad \bar{f}' = 0 \\ &\bar{\eta} \to \infty, \quad \bar{f}' \to 1. \end{aligned}\right\} \quad (23)$$

In equations (22) and (23) the primes denote differentiation with respect to the new independent variable $\bar{\eta}$.

It is important to realize that in the imaginary domain $\bar{f}_0$ and v_0 have the same sign, contrary to that in the real domain, so that the relationship corresponding to equation (20) is:

$$\bar{f}_0 = \frac{v_0}{\sqrt{[(\nu/\beta)(\mathrm{d}u_G/\mathrm{d}x)]}}. \quad (24)$$

2.3 *The Equation when β is Infinite*

(a) *When the variables are real*

Consider the relation between the parameter n in equation (12) and the parameter β in equation (18). When the parameter n passes through the value $n = 2$, equation (15) shows that β undergoes an infinite discontinuity, being large and positive when $n < 2$ and large and negative when $n > 2$. This case of infinite β was shown in Paper 2 to form the dividing line between the real and imaginary domains for solutions to equation (18).

Clearly, equation (18) cannot be used to evaluate numerical solutions for this case since the transformations defined by equations (16) and (17) are not then valid. The appropriate differential equation for this limiting case can, however, be deduced from equation (12).

If a new independent variable $\theta = (\zeta - \zeta_0)$ is introduced into equation (12), where ζ is defined in equation (9) and ζ_0 in equation (14), since ζ_0 is a constant, the equation becomes:

$$\frac{\mathrm{d}^3\theta}{\mathrm{d}\xi^3} + \left(1 - \frac{n}{2}\right)\theta\frac{\mathrm{d}^2\theta}{\mathrm{d}\xi^2} + k_0\frac{\mathrm{d}^2\theta}{\mathrm{d}\xi^2} + 1 - \left(\frac{\mathrm{d}\theta}{\mathrm{d}\xi}\right)^2 = 0 \quad (25)$$

where k_0 is a mass-transfer parameter defined by:

$$k_0 = \frac{-v_0}{[\nu(\mathrm{d}u_G/\mathrm{d}x)]^{1/2}}. \quad (26)$$

The differential equation for infinite β is then

obtained by putting $n = 2$ into equation (25), giving:

$$\frac{d^3\theta}{d\xi^3} + k_0 \frac{d^2\theta}{d\xi^2} + 1 - \left(\frac{d\theta}{d\xi}\right)^2 = 0, \quad (27)$$

and the boundary conditions associated with it are:

$$\left.\begin{aligned} &\xi = 0, \quad \theta = \frac{d\theta}{d\xi} = 0 \\ &\xi \to \infty, \quad \frac{d\theta}{d\xi} \to 1. \end{aligned}\right\} \quad (28)$$

Equation (27) with boundary conditions (28) holds when β tends to $+\infty$, from below in the real domain, or to $-\infty$, from above in the imaginary domain.

When no mass flows through the wall boundary, the parameter k_0 is zero and so is the second term in equation (27). The solution for this case is well-known and accurate values of the boundary-layer functions were given in Paper 7, Evans [3].

(b) *When the variables are imaginary*

When the velocity gradient du_G/dx is negative, the variables ξ and ζ defined in equations (8) and (9) are pure imaginary. The equation for infinite β for this case is again obtained by substituting in equation (27) new variables $\bar{\xi}$ and $\bar{\theta}$ defined by:

$$\left.\begin{aligned} \xi &= i\bar{\xi} \\ \theta &= i\bar{\theta} \end{aligned}\right\} \quad (29)$$

and replacing the constant k_0 by the constant $\bar{k}_0$ defined by:

$$k_0 = i\bar{k}_0. \quad (30)$$

This gives:

$$-\frac{d^3\bar{\theta}}{d\bar{\xi}^3} + \bar{k}_0 \frac{d^2\bar{\theta}}{d\bar{\xi}^2} + 1 - \left(\frac{d\bar{\theta}}{d\bar{\xi}}\right)^2 = 0 \quad (31)$$

with boundary conditions:

$$\left.\begin{aligned} &\bar{\xi} = 0, \quad \bar{\theta} = \frac{d\bar{\theta}}{d\bar{\xi}} = 0 \\ &\bar{\xi} \to \infty, \quad \frac{d\bar{\theta}}{d\bar{\xi}} \to 1. \end{aligned}\right\} \quad (32)$$

The relationship between the constant $\bar{k}_0$ and the velocity v_0 is:

$$\bar{k}_0 = \frac{v_0}{[\nu\,(du_G/dx)]^{1/2}}. \quad (33)$$

Equation (31) with boundary conditions (32) holds when β tends to $-\infty$, from above in the real domain, or to $+\infty$, from below in the imaginary domain.

3. RELATIONSHIPS BETWEEN FUNCTIONS OF THE VELOCITY LAYER

In Paper 2, Spalding and Evans [2], many formulae were given involving functions of the velocity boundary layer. Some of these formulae gave relationships between quantities which arise in similar solutions to the equations, while others enabled general boundary-layer functions to be deduced from exact similar solutions. General functions are those which, subject to the assumptions discussed in Paper 1, apply to *any* boundary layer whether similar or non-similar.

Some of these formulae which will be referred to in later sections are quoted below, but for detailed discussion the reader should consult Papers 1 and 2.

Boundary-layer thicknesses are first defined in terms of the similar length co-ordinate η by:

displacement thickness

$$\delta_1^* = \int_0^\infty \left(1 - \frac{df}{d\eta}\right) d\eta \quad (34)$$

momentum thickness

$$\delta_2 = \int_0^\infty \frac{df}{d\eta}\left(1 - \frac{df}{d\eta}\right) d\eta. \quad (35)$$

The present author has found that a "similar" boundary-layer thickness can be denoted by an asterisk whichever similar co-ordinates are used [i.e. whether they are (f, η) or (ζ, ξ) or any other]. This notation is brief and useful and does not in practice lead to confusion. This is partly because the groups, such as H_{14}, H_{12}, H_{24}, λ_2, F_2 or $v_0\delta_2/\nu$, which are finally required and, from experience, are the best groups with which to work, are independent of the similar co-ordinates used.

The relationship between these "similar" boundary-layer thicknesses and the corresponding physical thicknesses δ_1 and δ_2, which are

defined in terms of the length ν, is readily obtained from the appropriate "similar" transformation [e.g. equation (16)].

It is worth realizing that f_0'', being the wall shear in similar co-ordinates, can also be taken as the reciprocal of a "similar" shear thickness δ_4^*, although the more familiar symbol f_0'' will generally be used in the present work.

If equation (18) is integrated throughout the boundary layer, the following relationship is obtained:

$$-f_0'' + \int_0^\infty ff''\,\mathrm{d}\eta + \beta(\delta_1^* + \delta_2^*) = 0 \qquad (36)$$

where $f'' = 0$ in the main-stream and the definitions in equations (34) and (35) have been used. The second term in this can be integrated by parts to give:

$$\int_0^\infty ff''\,\mathrm{d}\eta = [ff']_0^\infty - \int^\infty f'^2\,\mathrm{d}\eta$$
$$= f(\infty) - \int_0^\infty f'^2\,\mathrm{d}\eta \qquad (37)$$

in which the boundary conditions in equation (19) have been used and $f(\infty)$ represents the value of the stream function in the main-stream. But this quantity can be written as:

$$f(\infty) = f_0 + \int_0^\infty f'\,\mathrm{d}\eta. \qquad (38)$$

On inserting equations (37) and (38) into equation (36), and rearranging, one obtains:

$$f_0'' = f_0 + \beta\delta_1^* + (\beta + 1)\,\delta_2^*. \qquad (39)$$

For $\beta = 0$, this equation gives the relationship between the quantities f_0, f_0'' and the momentum thickness δ_2^*, but the displacement thickness does not occur, whereas for the case $\beta = -1$ it relates f_0, f_0'' and δ_1^*, but the momentum thickness δ_2^* does not then appear.

Using the definitions already given, the functions required in the present work are obtained from the following formulae:

$$H_{12} = \frac{\delta_1^*}{\delta_2^*} \qquad (40)$$

$$H_{24} = f_0''\,\delta_2^* = \frac{\delta_2^*}{\delta_4^*} \qquad (41)$$

$$\frac{v_0\delta_2}{\nu} = -f_0\,\delta_2^*. \qquad (42)$$

When the functions occurring on the left-hand sides of these equations are evaluated for similar solutions (i.e. for given values of the parameter β), the pressure-gradient parameter relating to the momentum thickness is obtained from:

$$\lambda_2 \equiv \frac{\delta_2^2}{\nu}\frac{\mathrm{d}u_G}{\mathrm{d}x} = \frac{[H_{24} + (v_0\delta_2/\nu)]}{[1 + (1/\beta) + H_{12}]}. \qquad (43)$$

The function F_2, which measures the rate of growth of the momentum thickness, is then obtained from:

$$F_2 \equiv \frac{u_G}{\nu}\frac{\mathrm{d}\delta_2^2}{\mathrm{d}x} = 2\left\{\frac{1}{\beta} - 1\right\}\frac{[H_{24} - (v_0\delta_2/\nu)]}{[1 + (1/\beta) + H_{12}]}. \qquad (44)$$

The quantities occurring on the right-hand sides of equations (43) and (44) are evaluated from exact similar solutions, while the functions occurring on the left apply to any laminar boundary layer.

4. ASYMPTOTIC BEHAVIOUR OF BOUNDARY-LAYER FUNCTIONS FOR LARGE MASS-TRANSFER RATES

4.1 *General Discussion*

In this section, an examination is made of the behaviour of boundary-layer functions for high rates of mass flow through the wall boundary. Pretsch [4] has obtained some asymptotic values of thickness ratios for these conditions; his results were quoted in Paper 2 but since that paper was written the need has arisen for greater detail and higher accuracy.

For the well-known case of intensive suction, only sufficient detail will be given to show the form of the solution and the asymptotic values of the various functions. This case has been examined at length by Watson [5] who expressed the functions as asymptotic series in inverse powers of f_0^2; these series give high accuracy when f_0 is large. Watson considered only the real domain in detail but his formulae can be applied to the imaginary domain merely by replacing f_0^2 by $-f_0^2$ wherever it occurs.

The case of intensive blowing will be discussed in greater detail. The asymptotic form of the differential equation is first derived, and from this are obtained the asymptotic value of the wall shear f_0'' and relationships connecting the asymptotic values of the thickness ratios H_{14}, H_{12} and H_{24}. The last of these ratios is then

expressed in terms of gamma-functions, and a table of values of all three is given at convenient intervals in the parameter β. This table is more extensive and accurate than that given by Pretsch [4].

For ease of reference the formulae which hold for large mass-transfer rates are collected together in Appendix A.

4.2 *Intensive Suction*

Since the boundary layer becomes very thin for intensive inward mass flow, its behaviour may be examined by suitably extending the co-ordinates. Defining a new independent co-ordinate χ_1 and a new stream function φ_1 by:

$$\chi_1 = f_0 \eta \tag{45}$$

and

$$\varphi_1 = f_0(f - f_0), \tag{46}$$

equation (18) is transformed to:

$$\frac{\mathrm{d}^3\varphi_1}{\mathrm{d}\chi_1^3} + \frac{\mathrm{d}^2\varphi_1}{\mathrm{d}\chi_1^2} + \frac{1}{f_0^2}\left\{\varphi_1 \frac{\mathrm{d}^2\varphi_1}{\mathrm{d}\chi_1^2} + \beta\left[1 - \left(\frac{\mathrm{d}\varphi_1}{\mathrm{d}\chi_1}\right)^2\right]\right\} = 0 \tag{47}$$

with boundary conditions:

$$\left.\begin{aligned} &\chi_1 = 0, \quad \varphi_1 = \frac{\mathrm{d}\varphi_1}{\mathrm{d}\chi_1} = 0 \\ &\chi_1 \to \infty, \quad \frac{\mathrm{d}\varphi_1}{\mathrm{d}\chi_1} \to 1. \end{aligned}\right\} \tag{48}$$

The asymptotic form of equation (47) for large values of f_0 is clearly:

$$\frac{\mathrm{d}^3\varphi_1}{\mathrm{d}\chi_1^3} + \frac{\mathrm{d}^2\varphi_1}{\mathrm{d}\chi_1^2} = 0 \tag{49}$$

the solution of which, satisfying the boundary conditions in equation (48), is:

$$\varphi_1 = (\chi_1 - 1 + \mathrm{e}^{-\chi_1}). \tag{50}$$

From this, the distribution of velocity in the boundary layer is the well-known asymptotic suction profile:

$$\frac{u}{u_G} = (1 - \mathrm{e}^{-f_0\eta}). \tag{51}$$

For this profile it may be shown that the boundary-layer functions have the following values:

$$f_0'' = f_0 \tag{52}$$

$$\frac{v_0\delta_2}{\nu} = -\frac{1}{2} \tag{53}$$

$$H_{12} = 2 \tag{54}$$

$$H_{24} = \tfrac{1}{2} \tag{55}$$

$$H_{14} = 1 \tag{56}$$

$$\lambda_2 \equiv \frac{\delta_2^2}{\nu}\frac{\mathrm{d}u_G}{\mathrm{d}x} = 0 \tag{57}$$

$$F_2 \equiv \frac{u_G}{\nu}\frac{\mathrm{d}\delta_2^2}{\mathrm{d}x} = 0. \tag{58}$$

In solutions to equation (18), when the suction rate becomes very high the functions tend to these asymptotic values for all values of β, in the real and the imaginary domains.

4.3 *Intensive Blowing when β is Not Infinite*

4.31 *Transforming the differential equation*

It will have been noticed that the forms of the velocity equation in the real and the imaginary domains differ only in the sign of the first term. This, incidentally, means that a computer programme which has been prepared for obtaining solutions in the real domain requires only minor changes for use in the imaginary domain. To anticipate results to be given later, it will be found that for intensive blowing the first term in the differential equation becomes negligible, so that the equation assumes the same asymptotic form in the two domains. They can therefore be considered simultaneously, although the line separating the two domains, when the parameter β is infinite, must still be treated as a special case.

Since the first term in equation (18) becomes negligible, the resulting equation has the form obtained when the last term on the right-hand side of equation (1) vanishes. In other words, the case of intensive blowing behaves in some respects like that of negligibly small viscosity.

It is known that the boundary-layer thickness increases with increasing outward mass transfer. For high blowing rates, therefore, the boundary layer will become very thick, a fact which would

tend to contravene one of the fundamental assumptions of the theory that the boundary layer is confined to a very thin region near the wall. This does not affect the present discussion because here, and throughout the present series of papers, the approximation is assumed to hold. On the other hand, if the results for intensive blowing are to be applied to a practical problem it would be a wise precaution, before doing so, to test the validity of the boundary-layer approximation.

As the boundary layer is very thick its behaviour may be examined by making a suitable contraction of the co-ordinates. Defining a new independent variable χ and a new stream function φ by:

$$\chi = \frac{\eta}{f_0} \tag{59}$$

and

$$\varphi(\chi) = \frac{f}{f_0} \tag{60}$$

equation (18) becomes:

$$\frac{1}{f_0^2}\frac{\mathrm{d}^3\varphi}{\mathrm{d}\chi^3} + \varphi\frac{\mathrm{d}^2\varphi}{\mathrm{d}\chi^2} + \beta\left\{1 - \left(\frac{\mathrm{d}\varphi}{\mathrm{d}\chi}\right)^2\right\} = 0 \tag{61}$$

which for large f_0 reduces to:

$$\varphi\frac{\mathrm{d}^2\varphi}{\mathrm{d}\chi^2} + \beta\left\{1 - \left(\frac{\mathrm{d}\varphi}{\mathrm{d}\chi}\right)^2\right\} = 0. \tag{62}$$

This is clearly the asymptotic form for large rates of outward mass transfer of both equation (18), which holds in the real domain where β is positive in the range $0 \leqslant \beta < \infty$, and equation (22), which holds in the imaginary domain where β is negative in the range $-\infty < \beta < -0{\cdot}5$, although it does not hold when β is infinite.

In terms of these new variables, the boundary conditions given in equation (19) are:

$$\left.\begin{aligned} &\chi = 0, \quad \varphi = 1, \quad \frac{\mathrm{d}\varphi}{\mathrm{d}\chi} = 0 \\ &\chi \to \infty, \quad \frac{\mathrm{d}\varphi}{\mathrm{d}\chi} \to 1. \end{aligned}\right\} \tag{63}$$

These three boundary conditions are associated with the third-order differential equation (61). The general solution to the second-order equation (62) can, however, fulfil only two of these conditions, say the first two. It will be necessary later to put a further restriction on these solutions in order that they may behave like those of equation (61), satisfying all three boundary conditions.

4.32 *The asymptotic value of the wall shear* f_0''

When equation (62) is evaluated at the wall, it reduces to:

$$\left(\frac{\mathrm{d}^2\varphi}{\mathrm{d}\chi^2}\right)_0 + \beta = 0 \tag{64}$$

where the suffix denotes the wall value. If this is transformed back to the (η, f) co-ordinates using equations (59) and (60), it becomes:

$$f_0'' = -\frac{\beta}{f_0}. \tag{65}$$

In this relationship it should be remembered that for the real domain β is positive and f_0 is large and negative, whereas for the imaginary domain β is negative and f_0 is large and positive, so that f_0'' is always positive. When numerical solutions to equation (18) are examined it may be seen that equation (65) is a good approximation even for moderate blowing rates. For $\beta = 1$ in Table 2 (see section 6), for example, it holds to about 1 per cent when $f_0 = -3{\cdot}0$; for $f_0 = -4{\cdot}3346$, the most intensive blowing rate for the same value of β considered by Schlichting and Bussman [6] (see also Paper 2, Table 3), it holds to within 0·3 per cent.

Using equations (41) and (42) and the fact that $\lambda_2 = \beta(\delta_2^*)^2$, equation (65) may be written:

$$H_{24} = \frac{\nu}{v_0\delta_2} \cdot \lambda_2. \tag{66}$$

In other words, when the thickness ratio H_{24} is plotted as a function of the pressure-gradient parameter λ_2, with $v_0\delta_2/\nu$ as a parameter denoting the mass-transfer rate, lines of constant $v_0\delta_2/\nu$ are approximately linear, have the slope $(\nu/v_0\delta_2)$ and pass through the origin. Reference to Fig. 4(a) of Paper 2 shows that the lines for $(v_0\delta_2/\nu)$ equal to 2·0, 2·5 and 3·0 are gradually approaching this state, although the slopes of the lines have not quite reached their asymptotic values.

4.33 *Relationships between thickness ratios*

Some relationships which exist between the asymptotic values of the thickness ratios H_{14}, H_{12} and H_{24} will now be derived. On integrating equation (62) over the range $0 \leqslant \chi \leqslant \infty$, the following relationship is obtained:

$$\int_0^\infty \varphi \frac{d^2\varphi}{d\chi^2} d\chi + \beta \int_0^\infty \left(1 - \frac{d\varphi}{d\chi}\right) d\chi + \beta \int_0^\infty \frac{d\varphi}{d\chi}\left(1 - \frac{d\varphi}{d\chi}\right) d\chi = 0. \quad (67)$$

The first term in this can be integrated by parts to give:

$$\int_0^\infty \varphi \frac{d^2\varphi}{d\chi^2} d\chi = \left(\varphi \frac{d\varphi}{d\chi}\right)_0^\infty - \int_0^\infty \left(\frac{d\varphi}{d\chi}\right)^2 d\chi. \quad (68)$$

If, now, solutions to equation (62) are such as to satisfy the boundary condition $(d\varphi/d\chi) \to 1$ as $\chi \to \infty$, and the value of φ at large χ is written as:

$$\varphi(\infty) = \varphi_0 + \int_0^\infty \frac{d\varphi}{d\chi} d\chi, \quad (69)$$

substituting equation (69) into equation (68) and this in turn into equation (67) and using the facts that $d\chi = d\eta/f_0$ and $\varphi_0 = 1$ gives:

$$1 + \frac{\delta_2^*}{f_0} + \beta \frac{\delta_1^*}{f_0} + \beta \frac{\delta_2^*}{f_0} = 0 \quad (70)$$

where the boundary-layer thicknesses δ_1^* and δ_2^* have been defined in equations (34) and (35). It should be noted that equation (70) is the limiting value of equation (39) when f_0'' becomes very small.

Since the wall gradient f_0'' in equation (65) is the reciprocal of the shear thickness δ_4^*, the quantity f_0 occurring in equation (70) may be replaced by $-\beta\delta_4^*$, so that, after rearranging, the equation finally reduces to:

$$(1 - H_{14}) = \left(1 + \frac{1}{\beta}\right) H_{24} \quad (71)$$

where H_{14} and H_{24} are thickness ratios.

Equation (71) holds for all values of β, in the real domain, the imaginary domain, and even for infinite β, although the latter case was excluded from the discussion at the beginning of section 4.3. Two alternative forms of equation (71) are:

$$\left(\frac{1}{H_{24}} - H_{12}\right) = \left(1 + \frac{1}{\beta}\right) \quad (72)$$

and

$$\left(\frac{1}{H_{14}} - 1\right) = \frac{1}{H_{12}}\left(1 + \frac{1}{\beta}\right). \quad (73)$$

4.34 *Evaluating the thickness ratio H_{24}*

If one of the three thickness ratios can be evaluated exactly, the others can then be obtained from the above formulae. A convenient ratio to calculate is H_{24} which will be expressed in terms of gamma-functions.

If, for the moment, primes be used to denote differentiation with respect to χ, with the substitution:

$$\varphi'' = \varphi' \frac{d\varphi'}{d\varphi}, \quad (74)$$

equation (62) may be reduced to:

$$\frac{\varphi' \, d\varphi'}{(1 - \varphi'^2)} + \beta \frac{d\varphi}{\varphi} = 0 \quad (75)$$

which is readily integrable. After a short calculation, the velocity in the boundary layer may be expressed as:

$$\frac{d\varphi}{d\chi} = (1 - \varphi^{2\beta})^{1/2}. \quad (76)$$

The relationship between φ and χ will not be derived from this since it is not required here.

As we are restricting solutions to equation (62) so that the velocity $(d\varphi/d\chi)$ tends to unity at large distances from the wall, equation (76) must be interpreted differently in the real and the imaginary domains.

The real domain: In this case β is positive; therefore, in order that the velocity in the boundary layer may vary from zero at the wall to unity at the outer edge of the boundary layer, the function φ must decrease from unity at the wall to zero at the outer edge of the boundary layer. Because, as will be remembered, f_0 is large and negative, for asymptotic blowing the stream function f is negative throughout the boundary layer, becoming positive only at the point where the main-stream is reached. Solutions for $\beta = 1$, to be discussed in section 6,

show this clearly; in these the point at which the stream function changes sign gets closer to the main-stream as f_0 becomes more negative.

The imaginary domain: In this case the parameter β is negative and f_0 positive; the function q must therefore vary between unity at the wall and a large positive value at the outer edge of the boundary layer.

From the definition of χ in equation (59) and the relationship given in equation (65), the asymptotic value of H_{24} is:

$$H_{24} = -\beta \int_0^\infty \frac{dq}{d\chi}\left(1 - \frac{dq}{d\chi}\right) d\chi$$

$$= -\beta \int_1^{q(\infty)} \left(1 - \frac{dq}{d\chi}\right) dq \qquad (77)$$

where the upper limit $q(\infty)$ in the last expression is zero for the real domain and infinity for the imaginary domain.

Substituting equation (76) into (77) gives:

$$H_{24} = -\beta \int_1^{q(\infty)} \{1 - (1 - q^{2\beta})^{1/2}\}\, dq \qquad (78)$$

which, on introduction of a symbol for $q^{2\beta}$ and making a short calculation, gives finally for H_{24} the expression:

$$H_{24} = \beta - \frac{\pi^{1/2}}{4} \frac{\Gamma(1/2\beta)}{\Gamma[\frac{3}{2} - (1/2\beta)]} \qquad (79)$$

where Γ is the gamma-function. The second term on the right will be recognized as a "beta"-function but this symbol is not used in order to avoid confusion with β.

Equations (71–73) and (79) have been used to obtain the asymptotic values of the thickness ratios H_{14}, H_{12} and H_{24}. The results are contained in Table 1, but the case of infinite β will be considered before discussing this.

Table 1. Asymptotic values of thickness ratios for high blowing rates

β	H_{14}	H_{12}	H_{24}
0·0	0·0	∞	0·0
0·025	0·174409	8·66138	0·0201364
0·05	0·233775	6·40710	0·0364870
0·1	0·306349	4·85812	0·0630592
(1/9)	0·318404	4·67144	0·0681596
0·125	0·332143	4·47594	0·0742063
(1/7)	0·348017	4·27025	0·0814979
(1/6)	0·366667	4·05263	0·0904762
0·2	0·389049	3·82075	0·101825
0·25	0·416667	3·57143	0·116667
0·3	0·439174	3·39336	0·129421
(1/3)	0·452065	3·30013	0·136984
0·4	0·474019	3·15424	0·150280
0·5	0·500000	3·00000	0·166667
0·6	0·520251	2·89180	0·179906
0·8	0·549954	2·74949	0·200021
1·0	0·570796	2·65979	0·214602
1·2	0·586830	2·60390	0·225366
1·4	0·598249	2·55275	0·234355
1·6	0·607790	2·51818	0·241360
2·0	0·622058	2·46886	0·251962
3	0·642976	2·40124	0·267768
4	0·654370	2·36659	0·276504
5	0·661544	2·34551	0·282047
7	0·670087	2·32126	0·288674
10	0·676726	2·30268	0·293886
20	0·684772	2·28092	0·300218
$\pm\infty$	0·693147	2·25889	0·306853
−20	0·701862	2·23644	0·313829
−10	0·710987	2·21404	0·321126
− 7	0·719129	2·19459	0·327683
− 5	0·730480	2·16824	0·336900
− 4	0·740924	2·14490	0·345435
− 3	0·759497	2·10531	0·360754
− 2·0	0·801860	2·02347	0·396280
− 1·6	0·839367	1·95951	0·428355
− 1·4	0·870017	1·91238	0·454940
− 1·2	0·917336	1·84953	0·495984
− 1·0	1·000000	1·75194	0·570796
− 0·8	1·18558	1·59712	0·742323
− 0·7	1·40913	1·47609	0·954636
− 0·6	2·05719	1·29727	1·58579
− 0·55	3·32390	1·17025	2·84032
− 0·51	13·3414	1·03863	12·8451
− 0·50	∞	1·0	∞

4.4 *The Case when β is Infinite*

Of the two cases of infinite β considered in section 2.3, only equation (27), but not equation (31), has an asymptote for intensive blowing. The transformation:

$$\chi_2 = -\frac{\xi}{k_0} \qquad (80)$$

$$q_2 = -\frac{\theta}{k_0} \qquad (81)$$

is introduced into equation (27), the negative signs being used in order that χ_2 and q_2 may be positive, k_0 being, of course, a negative quantity. Equation (27) then becomes:

$$\frac{1}{k_0^2}\frac{d^3\varphi_2}{d\chi_2^3} - \frac{d^2\varphi_2}{d\chi_2^2} + 1 - \left(\frac{d\varphi_2}{d\chi_2}\right)^2 = 0. \quad (82)$$

For very large k_0, this is, after a change of sign,

$$\frac{d^2\varphi_2}{d\chi_2^2} - 1 + \left(\frac{d\varphi_2}{d\chi_2}\right)^2 = 0. \quad (83)$$

The boundary conditions given in equation (28) are:

$$\left.\begin{aligned} &\chi_2 = 0, \quad \varphi_2 = \frac{d\varphi_2}{d\chi_2} = 0 \\ &\chi_2 \to \infty, \quad \frac{d\varphi_2}{d\chi_2} \to 1. \end{aligned}\right\} \quad (84)$$

The solution to equation (83) is

$$\varphi_2 = \ln(\cosh \chi_2) \quad (85)$$

which, although a solution to a second-order equation, is seen to satisfy all three boundary conditions in equation (84).

From this solution, the second gradient of φ_2 at the wall is:

$$\left(\frac{d^2\varphi_2}{d\chi_2^2}\right)_0 = 1 \quad (86)$$

which, in terms of the function θ, is:

$$\left(\frac{d^2\theta}{d\xi^2}\right)_0 = -\frac{1}{k_0}. \quad (87)$$

Since the velocity distribution has the form:

$$\frac{d\varphi_2}{d\chi_2} = \tanh \chi_2, \quad (88)$$

by means of equation (87) the thickness ratio H_{24} becomes:

$$H_{24} = (1 - \ln 2) = 0{\cdot}306853. \quad (89)$$

Equations (71) and (72), which also hold for infinite β, are used to obtain the other ratios:

$$H_{14} = \ln 2 = 0{\cdot}693147 \quad (90)$$

and

$$H_{12} = \frac{\ln 2}{1 - \ln 2} = 2{\cdot}25889. \quad (91)$$

4.5 *Discussion of Table* 1

Table 1 contains the asymptotic values of the thickness ratios at convenient intervals in the parameter β. Some values of β are given as the reciprocal of an integer in order to specify them accurately but briefly. Most of the positive values of β included in the table are those occurring in earlier papers of the present series. The values additional to these were chosen either because the gamma-functions occurring in the formula for H_{24} in equation (79) are particularly easy to evaluate, which is the case when β is the reciprocal of an integer, or in order to obtain well-spaced values in the final thickness ratios. The ratios may be readily calculated for values of β not included in Table 1, from formulae already given, if comprehensive tables of gamma-functions are available.

Table 1 contains more values of β, and the thickness ratios are more accurate than the results given by Pretsch [4] which were contained in Table 4 of Paper 2. While there is good overall agreement with Pretsch's results, some individual values differ greatly from his.

In the present calculations, at least seven, usually eight, significant digits were used, with the aim of obtaining the final values accurate in the sixth digit. While most of the values in the table are believed to be as accurate as this, a few may contain an error of up to three units in the last digit quoted. This arises partly from the form of the relationships used to obtain the thickness ratios and partly from the methods used in the calculations, since many gamma-functions were evaluated from asymptotic formulae.

Examination of equation (79) shows that, when $\beta = -1/p$ where p is an integer equal to or greater than 2, the ratio H_{24} does not exist; when p is odd, the gamma-function in the denominator does not exist, and when p is even that in the numerator does not exist. An interpretation of this is that the velocity equation does not possess solutions for intensive blowing when the parameter β is equal to or lies beyond the point $\beta = -0{\cdot}5$. Mangler [7] also found that the equation has no solutions in the imaginary domain beyond this limiting value of β.

5. OBTAINING NUMERICAL SOLUTIONS ON A COMPUTER

A number of numerical solutions to equation (18) obtained on a computer will be given in

later sections. For numerical integration, the usual Runge–Kutta process was used. This process is well known, and most computers possess a standard programme for it. However, for purposes of reference both in the present paper and in later publications, and in order to supply the numerical coefficients employed, a brief description of the process is given in Appendix B.

In order to integrate throughout the boundary layer, accurate values of the wall shear f_0'' for specified values of the parameters β and f_0 were required. Where these were not known accurately, a number of trial runs was made to obtain them. The criterion employed for this was that the velocity f' should tend to unity as η became large and remain at that value.

When this happened, the stream function became a linear function of η for large η, and f'' became very small. For accurate solutions, the functions arrived at their final values in the following order as η increased: first the stream function became proportional to η, a few intervals later f' became unity and then after a few more intervals f'' became negligibly small.

When the starting value f_0'' was too small, the function f' increased to a maximum value, which was less than unity, and then, as f'' became negative, it began to decrease.

When f_0'' was too large, the function f' increased to values greater than unity as η increased.

For many values of β, particularly for negative values of f_0 in the real domain, the starting value f_0'' was required to extremely high accuracy in order to obtain a satisfactory solution.

6. THE FORWARD STAGNATION POINT FOR TWO-DIMENSIONAL FLOW; $\beta = 1$

The case when $\beta = 1$ in equation (18) corresponds to the forward stagnation point when the flow is two-dimensional. Some solutions for this case taken from the literature were quoted in Paper 2. Since these were in many respects inadequate for the present work, a new set of solutions was obtained.

The solutions are summarized in Table 2 and the distribution of the stream function and its first two derivatives are given in Table 2(a–m). The third derivative of f is not tabulated as it may be obtained by substituting f, f' and f'' into equation (18).

Preliminary values of f_0'' to four significant digits, from which more accurate values were obtained by successive approximation, were taken from Table 5 of Paper 2. The value for the case $f_0 = 0$ was already known to high accuracy from work done by Smith [8] (see also Paper 7 of the present series).

Since the present solutions were obtained, very accurate values of f_0'' as well as tables of the velocity distribution to four decimal places, have been found in a publication by Terrill [9].

Table 2. Solutions to the velocity equation for $\beta = 1{\cdot}0$, $-3{\cdot}0 \leqslant f_0 \leqslant 3{\cdot}0$

f_0	f_0''	δ_1^*	δ_2^*	$\frac{v_0\delta_2}{\nu}$	H_{12}	H_{24}	$\frac{\delta_2^2}{\nu}\frac{du_G}{dx}$	Solutions in Table
3·0	3·526640	0·26710	0·12977	−0·38931	2·0583	0·45765	0·016840	2(a)
2·5	3·091124	0·30072	0·14520	−0·36300	2·0711	0·44883	0·021083	2(b)
2·0	2·670056	0·34219	0·16393	−0·32786	2·0874	0·43770	0·026873	2(c)
1·5	2·267646	0·39399	0·18683	−0·28024	2·1088	0·42366	0·034905	2(d)
1·0	1·889314	0·45932	0·21500	−0·21500	2·1364	0·40620	0·046225	2(e)
0·5	1·541751	0·54233	0·24971	−0·12486	2·1718	0·38499	0·062355	2(f)
0·0	1·2325877	0·64789	0·29235	0·0	2·2161	0·36035	0·085469	2(g)
−0·5	0·9692296	0·78095	0·34414	0·17207	2·2693	0·33355	0·11843	2(h)
−1·0	0·75657486	0·94498	0·40580	0·40580	2·3287	0·30702	0·16467	2(i)
−1·5	0·59428178	1·13995	0·47717	0·71575	2·3890	0·28357	0·22769	2(j)
−2·0	0·4758098	1·36166	0·55708	1·11416	2·4443	0·26506	0·31034	2(k)
−2·5	0·390889090	1·60320	0·64384	1·60961	2·4900	0·25167	0·41454	2(l)
−3·0	0·3294530885	1·85839	0·73553	2·20659	2·5266	0·24232	0·54100	2(m)

Note that the solutions in the last three lines are less accurate than the others.

Table 2(a). *Solution for* $\beta = 1, f_0 = 3{\cdot}0$

η	f	f'	f''
0·0	3·00000	0·000000	3·526640
0·2	3·05718	0·514425	1·79541
0·4	3·18887	0·772133	0·881480
0·6	3·35728	0·896671	0·417484
0·8	3·54317	0·954734	0·190737
1·0	3·73708	0·980849	0·840470(−1)
1·2	3·93454	0·992177	0·357115(−1)
1·4	4·13352	0·996916	0·146284(−1)
1·6	4·33313	0·998827	0·577555(−2)
1·8	4·53298	0·999570	0·219743(−2)
2·0	4·73292	0·999848	0·805540(−3)
2·2	4·93291	0·999948	0·284489(−3)
2·4	5·13290	0·999983	0·967980(−4)
2·6	5·33290	0·999995	0·317479(−4)
2·8	5·53290	0·999999	0·100587(−4)
3·0	5·73290	1·00000	0·310279(−5)
3·2	5·93290	1·00000	0·958150(−6)
3·4	6·13290	1·00000	0·324257(−6)
3·6	6·33290	1·00000	0·145384(−6)
3·8	6·53290	1·00000	0·980222(−7)
4·0	6·73290	1·00000	0·871071(−7)

Table 2(b). *Solution for* $\beta = 1, f_0 = 2{\cdot}5$

η	f	f'	f''
0·0	2·50000	0·000000	3·091124
0·2	2·55153	0·469921	1·72599
0·4	2·67397	0·728135	0·930133
0·6	2·83478	0·865115	0·483942
0·8	3·01562	0·935279	0·243092
1·0	3·20656	0·969979	0·117866
1·2	3·40242	0·986542	0·551488(−1)
1·4	3·60059	0·994172	0·248936(−1)
1·6	3·79981	0·997563	0·108374(−1)
1·8	3·99949	0·999016	0·454921(−2)
2·0	4·19936	0·999617	0·184083(−2)
2·2	4·39931	0·999856	0·717886(−3)
2·4	4·59929	0·999948	0·269740(−3)
2·6	4·79928	0·999982	0·976150(−4)
2·8	4·99928	0·999994	0·339953(−4)
3·0	5·19928	0·999998	0·113677(−4)
3·2	5·39928	0·999999	0·362339(−5)
3·4	5·59928	1·00000	0·107217(−5)
3·6	5·79928	1·00000	0·262234(−6)
3·8	5·99928	1·00000	0·135466(−7)

Table 2(c). *Solution for* $\beta = 1, f_0 = 2{\cdot}0$

η	f	f'	f''
0·0	2·00000	0·000000	2·670056
0·2	2·04575	0·422915	1·63175
0·4	2·15799	0·677311	0·963435
0·6	2·30962	0·825203	0·549794
0·8	2·48379	0·908309	0·303231
1·0	2·67043	0·953445	0·161600
1·2	2·86375	0·977130	0·831884(−1)
1·4	3·06051	0·989135	0·413511(−1)
1·6	3·25900	0·995011	0·198410(−1)
1·8	3·45831	0·997786	0·918651(−2)
2·0	3·65801	0·999051	0·410318(−2)
2·2	3·85789	0·999608	0·176751(−2)
2·4	4·05784	0·999843	0·734154(−3)
2·6	4·25782	0·999940	0·294009(−3)
2·8	4·45781	0·999978	0·113549(−3)
3·0	4·65781	0·999992	0·423377(−4)
3·2	4·85780	0·999998	0·152979(−4)
3·4	5·05780	1·00000	0·542132(−5)
3·6	5·25780	1·00000	0·195396(−5)
3·8	5·45780	1·00000	0·786455(−6)
4·0	5·65780	1·00000	0·411864(−6)
4·2	5·85780	1·00000	0·300658(−6)
4·4	6·05780	1·00000	0·272665(−6)
4·6	6·25781	1·00000	0·270881(−6)

Table 2(d). *Solution for* $\beta = 1, f_0 = 1{\cdot}5$

η	f	f'	f''
0·0	1·50000	0·000000	2·267646
0·2	1·53991	0·373957	1·51237
0·4	1·64105	0·619538	0·975828
0·6	1·78178	0·775619	0·609408
0·8	1·94731	0·871640	0·368339
1·0	2·12786	0·928811	0·215413
1·2	2·31723	0·961745	0·121845
1·4	2·51160	0·980092	0·666300(−1)
1·6	2·70871	0·989972	0·352099(−1)
1·8	2·90727	0·995113	0·179725(−1)
2·0	3·10658	0·997697	0·885797(−2)
2·2	3·30626	0·998951	0·421388(−2)
2·4	3·50612	0·999538	0·193423(−2)
2·6	3·70606	0·999804	0·856402(−3)
2·8	3·90603	0·999919	0·365653(−3)
3·0	4·10602	0·999968	0·150508(−3)
3·2	4·30602	0·999988	0·597050(−4)
3·4	4·50602	0·999995	0·228152(−4)
3·6	4·70601	0·999998	0·839049(−5)
3·8	4·90601	0·999999	0·296208(−5)
4·0	5·10601	1·00000	0·995909(−6)
4·2	5·30601	1·00000	0·310290(−6)
4·4	5·50601	1·00000	0·797576(−7)
4·6	5·70601	1·00000	0·481469(−8)

Table 2(e). *Solution for* $\beta = 1, f_0 = 1{\cdot}0$

η	f	f'	f''
0·0	1·00000	0·000000	1·889314
0·2	1·03413	0·323946	1·36946
0·4	1·12341	0·555305	0·962117
0·6	1·25151	0·715513	0·655438
0·8	1·40611	0·823095	0·432947
1·0	1·57826	0·893138	0·277202
1·2	1·76165	0·937336	0·171953
1·4	1·95205	0·964352	0·103286
1·6	2·14666	0·980339	0·600409(−1)
1·8	2·34373	0·989494	0·337597(−1)
2·0	2·54219	0·994563	0·183516(−1)
2·2	2·74140	0·997278	0·963979(−2)
2·4	2·94102	0·998681	0·489100(−2)
2·6	3·14083	0·999383	0·239609(−2)
2·8	3·34075	0·999721	0·113307(−2)
3·0	3·54071	0·999878	0·517109(−3)
3·2	3·74069	0·999949	0·227789(−3)
3·4	3·94068	0·999980	0·969301(−4)
3·6	4·14068	0·999993	0·399512(−4)
3·8	4·34068	0·999998	0·160755(−4)
4·0	4·54068	1·00000	0·645408(−5)
4·2	4·74068	1·00000	0·273056(−5)
4·4	4·94068	1·00000	0·135405(−5)
4·6	5·14068	1·00000	0·874707(−6)
4·8	5·34068	1·00000	0·725260(−6)
5·0	5·54068	1·00000	0·692308(−6)

These include most, but not all, of the values of f_0 covered here, and in addition $f_0 = 4$, 5 and 10.

The numbers in the present tables are copies, after trivial changes were made in nomenclature, of the outputs given by the computer. Some values of f'' are given as a six-digit number multiplied by a large negative power of 10. The computer worked to fairly high accuracy, the ninth or tenth significant digit being correct, but even so it is very unlikely that the last significant digits in these very small values of f'' are correct. As it was not possible to estimate at which digit these values became inaccurate, the values given by the computer are given in the tables without change.

It is a common experience when equation (18) is solved numerically that solutions are considerably more difficult to obtain when mass transfer is outwards than when mass transfer is either absent or directed inwards. A way in which the difficulty manifests itself is that the wall gradient f_0'' for any given value of f_0 is required to very high accuracy, in order that the velocity f' may tend to unity for large η. This requirement becomes more severe as f_0 increases in magnitude.

The solutions for $f_0 = -2{\cdot}0$, $-2{\cdot}5$ and $-3{\cdot}0$ in Table 2(k), (l) and (m), respectively, show this clearly, where, although f_0'' was known to very high accuracy (an increase of one unit in the last digit quoted made the value too large), the velocity f' still did not quite become unity before f'' became negative. This difficulty has also been discussed by Eckert *et al.* [10].

Fortunately, these solutions are still useful, since it has been found that the error is quite small when they are used to evaluate such quantities as boundary-layer thicknesses in the velocity layer or the Nusselt number when calculating rates of heat transfer.

Table 2(f). *Solution for* $\beta = 1, f_0 = 0{\cdot}5$

η	f	f'	f''
0·0	0·500000	0·000000	1·541751
0·2	0·528538	0·274226	1·20746
0·4	0·605527	0·486047	0·918856
0·6	0·719436	0·645075	0·679676
0·8	0·860694	0·761134	0·488648
1·0	1·02164	0·843451	0·341318
1·2	1·19637	0·900164	0·231498
1·4	1·38046	0·938095	0·152361
1·6	1·57072	0·962707	0·972393(−1)
1·8	1·76494	0·978190	0·601385(−1)
2·0	1·96160	0·987626	0·360181(−1)
2·2	2·15973	0·993194	0·208774(−1)
2·4	2·35872	0·996373	0·117051(−1)
2·6	2·55819	0·998128	0·634426(−2)
2·8	2·75791	0·999065	0·332270(−2)
3·0	2·95778	0·999548	0·168079(−2)
3·2	3·15772	0·999789	0·820879(−3)
3·4	3·35769	0·999905	0·386927(−3)
3·6	3·55768	0·999958	0·175963(−3)
3·8	3·75767	0·999983	0·771833(−4)
4·0	3·95767	0·999993	0·326443(−4)
4·2	4·15767	0·999997	0·133087(−4)
4·4	4·35767	0·999999	0·522784(−5)
4·6	4·55767	1·00000	0·197706(−5)
4·8	4·75767	1·00000	0·718337(−6)
5·0	4·95767	1·00000	0·249244(−6)
5·2	5·15767	1·00000	0·809878(−7)
5·4	5·35767	1·00000	0·228445(−7)
5·6	5·55767	1·00000	0·345096(−8)

7. SOLUTIONS FOR $\beta = -1$

When $\beta = -1$ in equation (18), a simple relationship was found between the wall shear f_0'' and the mass-transfer parameter f_0. This means that, in a computer programme for solving the equation numerically, the starting values f_0 and f_0'' can be specified exactly without the need for successive approximation.

The exceptional behaviour of the case $\beta = -1$ was first observed by Thwaites [11–13] who integrated the differential equation in terms of error functions. This work was brought to the notice of the author only after preparation of the present paper. It should be possible to draw up a more accurate and complete set of functions from an exact solution of this nature than was possible by the numerical methods employed here.

Table 2(g). *Solution for* $\beta = 1, f_0 = 0$

η	f	f'	f''
0·0	0·0000000	0·000000	1·2325877
0·2	0·0233223	0·226612	1·03445
0·4	0·0880566	0·414456	0·846326
0·6	0·186701	0·566281	0·675172
0·8	0·312423	0·685938	0·525132
1·0	0·459227	0·777865	0·398013
1·2	0·622028	0·846671	0·293776
1·4	0·796652	0·896809	0·211003
1·6	0·979780	0·932348	0·147352
1·8	1·16886	0·956834	0·999641(−1)
2·0	1·36197	0·973217	0·658257(−1)
2·2	1·55776	0·983854	0·420400(−1)
2·4	1·75525	0·990550	0·260207(−1)
2·6	1·95381	0·994634	0·155977(−1)
2·8	2·15300	0·997046	0·904929(−2)
3·0	2·35256	0·998425	0·507841(−2)
3·2	2·55233	0·999187	0·275536(−2)
3·4	2·75221	0·999594	0·144470(−2)
3·6	2·95215	0·999804	0·731783(−3)
3·8	3·15212	0·999909	0·358039(−3)
4·0	3·35211	0·999960	0·169252(−3)
4·2	3·55211	0·999983	0·773960(−4)
4·4	3·75210	0·999994	0·343594(−4)
4·6	3·95210	0·999998	0·149530(−4)
4·8	4·15210	1·00000	0·653871(−5)
5·0	4·35210	1·00000	0·303872(−5)
5·2	4·55210	1·00000	0·165020(−5)
5·4	4·75210	1·00000	0·113338(−5)
5·6	4·95210	1·00000	0·962240(−6)
5·8	5·15210	1·00000	0·922646(−6)

Table 2(h). *Solution for* $\beta = 1, f_0 = -0{\cdot}5$

η	f	f'	f''
0·0	−0·500000	0·000000	0·9692296
0·2	−0·481318	0·183247	0·862040
0·4	−0·428168	0·344526	0·750471
0·6	−0·344997	0·483482	0·639574
0·8	−0·236228	0·600675	0·533436
1·0	−0·106094	0·697385	0·435188
1·2	0·0414808	0·775424	0·347020
1·4	0·202975	0·836953	0·270234
1·6	0·375317	0·884310	0·205312
1·8	0·555911	0·919856	0·152035
2·0	0·742623	0·945849	0·109619
2·2	0·933752	0·964349	0·768798(−1)
2·4	1·12798	0·977152	0·523963(−1)
2·6	1·32433	0·985758	0·346704(−1)
2·8	1·52209	0·991373	0·222545(−1)
3·0	1·72075	0·994927	0·138465(−1)
3·2	1·91997	0·997105	0·834479(−2)
3·4	2·11953	0·998399	0·486823(−2)
3·6	2·31929	0·999142	0·274771(−2)
3·8	2·51917	0·999556	0·149980(−2)
4·0	2·71910	0·999778	0·791528(−3)
4·2	2·91907	0·999894	0·403972(−3)
4·4	3·11905	0·999952	0·199597(−3)
4·6	3·31905	0·999980	0·957723(−4)
4·8	3·51905	0·999994	0·449898(−4)
5·0	3·71904	1·00000	0·210984(−4)
5·2	3·91905	1·00000	0·103092(−4)
5·4	4·11905	1·00000	0·565512(−5)
5·6	4·31905	1·00001	0·376215(−5)

7.1 *The Real Domain*

For $\beta = -1$, equation (18) has the form:

$$f''' + ff'' - 1 + f'^2 = 0 \qquad (92)$$

On combination of the second and last terms on the left-hand side, two integrations and insertion of the boundary conditions at the wall given in equation (19), this reduces to:

$$2\frac{df}{d\eta} + f^2 = f_0^2 + 2f_0''\eta + \eta^2 \qquad (93)$$

with the remaining boundary condition:

$$\frac{df}{d\eta} \to 1 \text{ exponentially as } \eta \to \infty. \qquad (94)$$

In the definition of the displacement thickness δ_1^* in equation (34), the contribution of large values of η to the integral is very small. It is

Table 2(i). *Solution for* $\beta = 1, f_0 = -1{\cdot}0$

η	f	f'	f''
0·0	−1·000000	0·000000	0·75657486
0·2	−0·985208	0·146144	0·703457
0·4	−0·942302	0·280906	0·643189
0·6	−0·873684	0·403109	0·578262
0·8	−0·781943	0·512058	0·511033
1·0	−0·669762	0·607514	0·443673
1·2	−0·539827	0·689649	0·378130
1·4	−0·394755	0·758999	0·316076
1·6	−0·237024	0·816403	0·258865
1·8	−0·0689186	0·862936	0·207496
2·0	0·107508	0·899834	0·162594
2·2	0·290461	0·928422	0·124408
2·4	0·478412	0·950039	0·928400(−1)
2·6	0·670098	0·965973	0·674959(−1)
2·8	0·864502	0·977411	0·477530(−1)
3·0	1·06083	0·985397	0·328442(−1)
3·2	1·25849	0·990815	0·219398(−1)
3·4	1·45704	0·994385	0·142212(−1)
3·6	1·65616	0·996666	0·893741(−2)
3·8	1·85564	0·998079	0·544174(−2)
4·0	2·05535	0·998927	0·320791(−2)
4·2	2·25519	0·999419	0·182981(−2)
4·4	2·45511	0·999695	0·100941(−2)
4·6	2·65506	0·999846	0·538329(−3)
4·8	2·85504	0·999925	0·277501(−3)
5·0	3·05503	0·999965	0·138302(−3)
5·2	3·25502	0·999984	0·667200(−4)
5·4	3·45502	0·999994	0·312651(−4)
5·6	3·65502	0·999998	0·143598(−4)
5·8	3·85502	1·00000	0·660797(−5)
6·0	4·05502	1·00000	0·319709(−5)
6·2	4·25502	1·00000	0·176529(−5)
6·4	4·45502	1·00000	0·120036(−5)
6·6	4·65502	1·00000	0·100016(−5)
6·8	4·85502	1·00000	0·947571(−6)
7·0	5·05502	1·00000	0·951021(−6)

Table 2(j). *Solution for* $\beta = 1, f_0 = -1{\cdot}5$

η	f	f'	f''
0·0	−1·50000	0·000000	0·59428178
0·2	−1·48827	0·116475	0·569456
0·4	−1·45378	0·227408	0·539018
0·6	−1·39775	0·331771	0·503909
0·8	−1·32157	0·428726	0·465114
1·0	−1·22679	0·517638	0·423644
1·2	−1·11508	0·598074	0·380526
1·4	−0·988142	0·669807	0·336787
1·6	−0·847736	0·732814	0·293427
1·8	−0·695587	0·787267	0·251397
2·0	−0·533376	0·833519	0·211561
2·2	−0·362692	0·872087	0·174659
2·4	−0·185010	0·903618	0·141281
2·6	−0·00166414	0·928861	0·111827
2·8	0·186169	0·948625	0·865024(−1)
3·0	0·377476	0·963738	0·653100(−1)
3·2	0·571408	0·975013	0·480700(−1)
3·4	0·767276	0·983208	0·344516(−1)
3·6	0·964532	0·989006	0·240166(−1)
3·8	1·16276	0·992994	0·162681(−1)
4·0	1·36164	0·995658	0·106975(−1)
4·2	1·56096	0·997386	0·682286(−2)
4·4	1·76055	0·998472	0·421747(−2)
4·6	1·96032	0·999133	0·252479(−2)
4·8	2·16019	0·999524	0·146288(−2)
5·0	2·36012	0·999746	0·819877(−3)
5·2	2·56008	0·999869	0·444252(−3)
5·4	2·76006	0·999935	0·232634(−3)
5·6	2·96005	0·999969	0·117696(−3)
5·8	3·16005	0·999986	0·575298(−4)
6·0	3·36005	0·999994	0·271849(−4)
6·2	3·56005	0·999997	0·124439(−4)
6·4	3·76005	0·999999	0·554944(−5)
6·6	3·96005	1·00000	0·244687(−5)
6·8	4·16005	1·00000	0·110574(−5)
7·0	4·36005	1·00000	0·550794(−6)
7·2	4·56005	1·00000	0·332961(−6)

therefore possible to specify δ_1^* to any required accuracy by replacing the upper limit by some large value η_1 of η beyond which the contribution to the integral is negligible. When this is done and the integration is carried out, the following result ensues:

$$\delta_1^* = \int_0^{\eta_1} \left(1 - \frac{\mathrm{d}f}{\mathrm{d}\eta}\right)\mathrm{d}\eta = \eta_1 - f(\eta_1) + f_0. \quad (95)$$

At sufficiently large distances from the wall, therefore, the stream function may be written accurately as:

$$f(\eta_1) = (\eta_1 + f_0 - \delta_1^*)_{\eta_1 \text{ large}}. \quad (96)$$

Substituting this and the boundary condition (94) into equation (93) then gives:

$$\delta_1^{*2} - 2f_0\delta_1^* + 2 + 2(f_0 - \delta_1^* - f_0'')\,\eta_1 = 0. \quad (97)$$

Since this holds for any large value of η_1, both the coefficient of η_1 and the group of terms which are not multiplied by η_1 must be identically zero. The following relationships therefore hold:

$$f_0'' = f_0 - \delta_1^* \quad (98)$$

and

$$\delta_1^* = f_0 \pm (f_0^2 - 2)^{1/2}. \qquad (99)$$

Equation (98) is clearly equation (39) for the present value of β.

From these equations the wall gradient f_0'' is then related to the parameter f_0 by:

$$f_0'' = (f_0^2 - 2)^{1/2} \qquad (100)$$

the positive sign in equation (99) having been used for obvious reasons.

Using this relationship, exact corresponding values of f_0 and f_0'' were used in obtaining numerical solutions to equation (18) on a computer. These solutions are summarized in Table 3 and the distributions with η of the stream function f and its first two derivatives are given in Table 3(a–h). The magnitudes of f_0 were chosen so as to give well-spaced values for the mass-transfer parameter $(v_0\delta_2/\nu)$ between −0·58559, its value at the separation point, and −0·5, the value when f_0 is infinite.

Table 2(k). *Solution for* $\beta = 1, f_0 = -2{\cdot}0$

η	f	f'	f''
0·0	−2·00000	0·0000000	0·4758098
0·2	−1·99056	0·0940678	0·464244
0·4	−1·96255	0·185459	0·449089
0·6	−1·91660	0·273485	0·430655
0·8	−1·85342	0·357525	0·409283
1·0	−1·77389	0·437028	0·385345
1·2	−1·67895	0·511519	0·359245
1·4	−1·56964	0·580610	0·331418
1·6	−1·44708	0·644002	0·302332
1·8	−1·31243	0·701493	0·272483
2·0	−1·16689	0·752980	0·242392
2·2	−1·01164	0·798469	0·212592
2·4	−0·847890	0·838072	0·183616
2·6	−0·676791	0·872004	0·155977
2·8	−0·499446	0·900583	0·130145
3·0	−0·316888	0·924209	0·106516
3·2	−0·130061	0·943357	0·853946(−1)
3·4	0·0601913	0·958547	0·669703(−1)
3·6	0·253131	0·970329	0·513086(−1)
3·8	0·448133	0·979251	0·383525(−1)
4·0	0·644676	0·985840	0·279356(−1)
4·2	0·842345	0·990578	0·198050(−1)
4·4	1·04081	0·993893	0·136511(−1)
4·6	1·23983	0·996148	0·913861(−2)
4·8	1·43922	0·997636	0·593577(−2)
5·0	1·63885	0·998589	0·373695(−2)
5·2	1·83863	0·999180	0·227781(−2)
5·4	2·03851	0·999535	0·134236(−2)
5·6	2·23844	0·999741	0·763221(−3)
5·8	2·43840	0·999856	0·417069(−3)
6·0	2·63838	0·999917	0·217330(−3)
6·2	2·83836	0·999948	0·106014(−3)
6·4	3·03835	0·999963	0·460190(−4)
6·6	3·23835	0·999969	0·146521(−4)
6·8	3·43834	0·999970	−0·136784(−5)

Table 2(l). *Solution for* $\beta = 1, f_0 = -2{\cdot}5$

η	f	f'	f''
0·0	−2·50000	0·0000000	0·390889090
0·2	−2·49222	0·0776471	0·385209
0·4	−2·46903	0·153938	0·377343
0·6	−2·43076	0·228445	0·367393
0·8	−2·37780	0·300764	0·355477
1·0	−2·31063	0·370514	0·341724
1·2	−2·22979	0·437341	0·326278
1·4	−2·13591	0·500923	0·309299
1·6	−2·02966	0·560970	0·290962
1·8	−1·91177	0·617230	0·271463
2·0	−1·78303	0·669492	0·251017
2·2	−1·64425	0·717589	0·229863
2·4	−1·49628	0·761407	0·208263
2·6	−1·33998	0·800884	0·186507
2·8	−1·17622	0·836020	0·164901
3·0	−1·00586	0·866876	0·143772
3·2	−0·829742	0·893582	0·123445
3·4	−0·648687	0·916329	0·104241
3·6	−0·463458	0·935372	0·864469(−1)
3·8	−0·274765	0·951018	0·703060(−1)
4·0	−0·0832534	0·963617	0·559950(−1)
4·2	0·110504	0·973545	0·436128(−1)
4·4	0·306013	0·981192	0·331742(−1)
4·6	0·502854	0·986940	0·246119(−1)
4·8	0·700686	0·991153	0·177876(−1)
5·0	0·899235	0·994158	0·125088(−1)
5·2	1·09829	0·996244	0·855007(−2)
5·4	1·29769	0·997651	0·567473(−2)
5·6	1·49732	0·998571	0·365362(−2)
5·8	1·69709	0·999155	0·227980(−2)
6·0	1·89696	0·999514	0·137733(−2)
6·2	2·09689	0·999728	0·804720(−3)
6·4	2·29685	0·999851	0·453943(−3)
6·6	2·49683	0·999919	0·246544(−3)
6·8	2·69681	0·999955	0·128205(−3)
7·0	2·89681	0·999974	0·630291(−4)
7·2	3·09680	0·999983	0·283528(−4)
7·4	3·29680	0·999986	0·104921(−4)
7·6	3·49680	0·999987	0·154128(−5)
7·8	3·69680	0·999987	−0·287245(−5)
8·0	3·89679	0·999986	−0·506581(−5)

Table 2(m). *Solution for* $\beta = 1, f_0 = -3{\cdot}0$

η	f	f'	f''
0·0	−3·00000	0·0000000	0·3294530885
0·2	−2·99343	0·0656115	0·326432
0·4	−2·97381	0·130482	0·322047
0·6	−2·94130	0·194342	0·316338
0·8	−2·89615	0·256932	0·309349
1·0	−2·83863	0·318000	0·301131
1·2	−2·76907	0·377306	0·291738
1·4	−2·68784	0·434621	0·281233
1·6	−2·59537	0·489729	0·269684
1·8	−2·49211	0·542430	0·257164
2·0	−2·37857	0·592536	0·243757
2·2	−2·25528	0·639879	0·229553
2·4	−2·12281	0·684311	0·214654
2·6	−1·98176	0·725702	0·199175
2·8	−1·83274	0·763951	0·183245
3·0	−1·67639	0·798980	0·167011
3·2	−1·51337	0·830746	0·150642
3·4	−1·34431	0·859240	0·134323
3·6	−1·16989	0·884492	0·118259
3·8	−0·990728	0·906575	0·102668
4·0	−0·807461	0·925606	0·877707(−1)
4·2	−0·620679	0·941744	0·737839(−1)
4·4	−0·430942	0·955193	0·609021(−1)
4·6	−0·238765	0·966190	0·492856(−1)
4·8	−0·0446124	0·974999	0·390465(−1)
5·0	0·151107	0·981904	0·302400(−1)
5·2	0·348041	0·987190	0·228608(−1)
5·4	0·545894	0·991139	0·168453(−1)
5·6	0·744425	0·994012	0·120806(−1)
5·8	0·943443	0·996045	0·841788(−2)
6·0	1·14280	0·997441	0·568780(−2)
6·2	1·34239	0·998371	0·371614(−2)
6·4	1·54213	0·998967	0·233715(−2)
6·6	1·74196	0·999335	0·140324(−2)
6·8	1·94185	0·999550	0·790534(−3)
7·0	2·14177	0·999666	0·400607(−3)
7·2	2·34171	0·999720	0·159173(−3)
7·4	2·54166	0·999736	0·128599(−4)
7·6	2·74161	0·999729	−0·748929(−4)

In Table 3, the quantities f_0, f_0'' and δ_1^* are written as square roots in order to specify them to high accuracy.

In Table 3(a–h), the interval in η is in some cases 0·1 and in others 0·2. Since the initial values of f_0 and f_0'' were specified to ten significant digits, it is expected that these tables are accurate to six digits, with the possible exception of the values of f'' less than $1{\cdot}0 \times 10^{-4}$ which are probably only accurate in the first few significant digits.

7.2 *The Imaginary Domain*

It is clear that the case $\beta = -1$ also contains special features in the imaginary domain. By means of the same method as used for the real domain some numerical solutions have also been obtained for this case. However, since they show some unexpected features which require fuller discussion than is possible here, they will be published elsewhere.

8. SOLUTIONS IN THE REAL DOMAIN FOR HIGH VALUES OF β WHEN $f_0 = 0$

Solutions in the real domain when no mass flows through the wall boundary were quoted in Paper 7, Evans [3]. They were given to high accuracy and were largely taken from calculations by Smith [8]. With suitably small intervals in the parameter β, they covered the range from the separation point at $\beta = -0{\cdot}198838$ to the value $\beta = 2$. The solution for $\beta = \infty$, which is known in closed form, was also given, but a large gap, where no exact solutions were known, still remained between $\beta = 2$ and $\beta = \infty$.

Some interpolated solutions for this region,

Table 3. *Solutions to the velocity equation in the real domain for* $\beta = -1{\cdot}0$

f_0	f_0''	δ_1^*	δ_2^*	$\frac{v_0\delta_2}{\nu}$	H_{12}	H_{24}	$\lambda_2 = \frac{\delta_2^2}{\nu}\frac{du_G}{dx}$	$F_2 = \frac{u_G}{\nu}\frac{d\delta_2^2}{dx}$	Solution in Table
$(2)^{\frac{1}{2}}$	0	$(2)^{\frac{1}{2}}$	0·41407	−0·58559	3·4154	0·0	−0·17146	0·68582	3(a)
$(25/12)^{\frac{1}{2}}$	$(1/12)^{\frac{1}{2}}$	$(4/3)^{\frac{1}{2}}$	0·39954	−0·57668	2·8901	0·11534	−0·15963	0·63852	3(b)
$(20/9)^{\frac{1}{2}}$	$(2/9)^{\frac{1}{2}}$	$(20/9)^{\frac{1}{2}} - (2/9)^{\frac{1}{2}}$	0·38017	−0·56672	2·6812	0·17921	−0·14453	0·57812	3(c)
$(5/2)^{\frac{1}{2}}$	$(1/2)^{\frac{1}{2}}$	$(5/2)^{\frac{1}{2}} - (1/2)^{\frac{1}{2}}$	0·35026	−0·55381	2·4954	0·24767	−0·12268	0·49073	3(d)
$(3)^{\frac{1}{2}}$	1	$(3)^{\frac{1}{2}} - 1$	0·31200	−0·54041	2·3463	0·31200	−0·097347	0·38939	3(e)
2	$(2)^{\frac{1}{2}}$	$2 - (2)^{\frac{1}{2}}$	0·26359	−0·52717	2·2224	0·37277	0·069477	0·27791	3(f)
$(5)^{\frac{1}{2}}$	$(3)^{\frac{1}{2}}$	$(5)^{\frac{1}{2}} - (3)^{\frac{1}{2}}$	0·23279	−0·52053	2·1651	0·40320	−0·054191	0·21676	3(g)
$(10)^{\frac{1}{2}}$	$(8)^{\frac{1}{2}}$	$(10)^{\frac{1}{2}} - (8)^{\frac{1}{2}}$	0·16105	−0·50929	2·0730	0·45552	−0·025937	0·10375	3(h)
∞	∞	—	—	−0·5	2·0	0·5	0·0	0·0	—

Table 3(a). *Solution for* $\beta = -1, f_0 = (2)^{\frac{1}{2}}$

η	f	f'	f''
0·0	1·414213562	0·00000000	0·000000
0·1	1·41437	0·00477240	0·932500(−1)
0·2	1·41546	0·0182398	0·174182
0·3	1·41827	0·0392499	0·244333
0·4	1·42353	0·0667881	0·304925
0·5	1·43182	0·0999477	0·356893
0·6	1·44367	0·137902	0·400914
0·7	1·45953	0·179882	0·437457
0·8	1·47976	0·225155	0·466825
0·9	1·50465	0·273014	0·489210
1·0	1·53443	0·322768	0·504737
1·1	1·56924	0·373736	0·513517
1·2	1·60919	0·425251	0·515690
1·3	1·65429	0·476661	0·511464
1·4	1·70450	0·527341	0·501148
1·5	1·75972	0·576702	0·485170
1·6	1·81978	0·624204	0·464087
1·7	1·88448	0·669372	0·438584
1·8	1·95356	0·711800	0·409455
1·9	2·02674	0·751171	0·377575
2·0	2·10369	0·787254	0·343865
2·1	2·18407	0·819914	0·309249
2·2	2·26755	0·849103	0·274614
2·3	2·35378	0·874863	0·240767
2·4	2·44241	0·897307	0·208406
2·5	2·53314	0·916613	0·178096
2·6	2·62564	0·933008	0·150257
2·7	2·71965	0·946755	0·125158
2·8	2·81491	0·958136	0·102932
2·9	2·91121	0·967438	0·835881(−1)
3·0	3·00834	0·974946	0·670304(−1)
3·1	3·10615	0·980931	0·530853(—1)
3·2	3·20448	0·985643	0 415238(−1)
3·3	3·30324	0·989307	0·320838(−1)
3·4	3·40232	0·992121	0·244899(−1)
3·5	3·50164	0·994257	0·184692(−1)
3·6	3·60115	0·995859	0·137631(−1)
3·7	3·70080	0·997046	0·101353(−1)
3·8	3·80055	0·997915	0·737646(−2)
3·9	3·90037	0·998544	0·530635(−2)
4·0	4·00025	0·998994	0·377327(−2)
4·1	4·10017	0·999312	0·265247(−2)
4·2	4·20011	0·999535	0·184344(−2)
4·3	4·30007	0·999689	0·126673(−2)
4·4	4·40005	0·999794	0·860686(—3)
4·5	4·50003	0·999865	0·578283(−3)
4·6	4·60002	0·999912	0·384235(−3)
4·7	4·70001	0·999944	0·252486(−3)
4·8	4·80001	0·999964	0·164091(−3)
4·9	4·90001	0·999978	0·105478(−3)
5·0	5·00000	0·999986	0·670630(−4)
5·1	5·10000	0·999991	0·421765(−4)
5·2	5·20000	0·999995	0·262385(−4)
5·3	5·30000	0·999997	0·161475(−4)
5·4	5·40000	0·999998	0·983062(−5)
5·5	5·50000	0·999999	0·592078(−5)
5·6	5·60000	0·999999	0·352787(−5)
5·7	5·70000	1·00000	0·207966(−5)
5·8	5·80000	1·00000	0·121289(−5)
5·9	5·90000	1·00000	0·699822(−6)
6·0	6·00000	1·00000	0·399478(−6)

Table 3(b). *Solution for* $\beta = -1, f_0 = (25/12)^{\frac{1}{2}}$

η	f	f'	f''
0·0	1·443375672	0·0000000	0·288675135
0·2	1·44987	0·0683357	0·389597
0·4	1·47186	0·153951	0·462082
0·6	1·51224	0·251431	0·508450
0·8	1·57288	0·355630	0·529311
1·0	1·65461	0·461482	0·525105
1·2	1·75726	0·564102	0·497404
1·4	1·87974	0·659107	0·449728
1·6	2·02016	0·743029	0·387640
1·8	2·17606	0·813665	0·318092
2·0	2·34468	0·870246	0·248223
2·2	2·52326	0·913341	0·184082
2·4	2·70923	0·944536	0·129714
2·6	2·90042	0·965999	0·868702(−1)
2·8	3·09513	0·980040	0·553227(−1)
3·0	3·29209	0·988780	0·335282(−1)
3·2	3·49041	0·993959	0·193532(−1)
3·4	3·68952	0·996885	0·106489(−1)
3·6	3·88907	0·998461	0·558998(−2)
3·8	4·08885	0·999271	0·280153(−2)
4·0	4·28875	0·999669	0·134135(−2)
4·2	4·48871	0·999856	0·613906(−3)
4·4	4·68869	0·999940	0·268714(−3)
4·6	4·88868	0·999976	0·112537(−3)
4·8	5·08868	0·999991	0·451112(−4)
5·0	5·28868	0·999997	0·173140(−4)
5·2	5·48868	0·999999	0·636452(−5)
5·4	5·68868	1·00000	0·224130(−5)
5·6	5·88868	1·00000	0·756239(−6)
5·8	6·08868	1·00000	0·244573(−6)
6·0	6·28868	1·00000	0·758728(−7)

in the form of values of the thickness ratios H_{12} and H_{24}, were given in Paper 2. The method by which the interpolated solutions were obtained should have given an accuracy of about $\pm 0{\cdot}3$ per cent. The present, more accurate calculations have shown that the values of H_{12} were all slightly less than 0·1 per cent low, while

Table 3(c). *Solution for* $\beta = -1, f_0 = (20/9)^{\frac{1}{2}}$

η	f	f'	f''
0·0	1·490711985	0·0000000	0·4714045209
0·2	1·50051	0·0996318	0·521906
0·4	1·53112	0·207516	0·553674
0·6	1·58380	0·319738	0·565003
0·8	1·65902	0·432065	0·554602
1·0	1·75635	0·540142	0·522729
1·2	1·87452	0·639889	0·471922
1·4	2·01152	0·727971	0·407076
1·6	2·16478	0·802221	0·334773
1·8	2·33143	0·861854	0·262051
2·0	2·50858	0·907427	0·195049
2·2	2·69357	0·940542	0·137989
2·4	2·88412	0·963418	0·927943(−1)
2·6	3·07841	0·978446	0·593432(−1)
2·8	3·27512	0·987838	0·361153(−1)
3·0	3·47330	0·993428	0·209330(−1)
3·2	3·67233	0·996598	0·115653(−1)
3·4	3·87184	0·998313	0·609552(−2)
3·6	4·07160	0·999198	0·306704(−2)
3·8	4·27149	0·999635	0·147424(−2)
4·0	4·47144	0·999841	0·677346(−3)
4·2	4·67142	0·999933	0·297621(−3)
4·4	4·87141	0·999973	0·125118(−3)
4·6	5·07141	0·999990	0·503431(−4)
4·8	5·27141	0·999996	0·193941(−4)
5·0	5·47141	0·999999	0·715539(−5)
5·2	5·67141	1·00000	0·252881(−5)
5·4	5·87141	1·00000	0·856092(−6)
5·6	6·07141	1·00000	0·277524(−6)
5·8	6·27141	1·00000	0·859445(−7)
6·0	6·47141	1·00000	0·252226(−7)
6·2	6·67141	1·00000	0·683622(−8)
6·4	6·87140	1·00000	0·176441(−8)
6·6	7·07140	1·00000	0·437694(−9)
6·8	7·27140	1·00000	0·104325(−9)
7·0	7·47140	1·00000	0·238918(−10)
7·2	7·67140	1·00000	0·525725(−11)

Table 3(d). *Solution for* $\beta = -1, f_0 = (5/2)^{\frac{1}{2}}$

η	f	f'	f''
0·0	1·581138830	0·0000000	0·7071067810
0·1	1·58466	0·0701444	0·695952
0·2	1·59513	0·139199	0·685066
0·3	1·61246	0·207122	0·673131
0·4	1·63651	0·273755	0·659103
0·5	1·66716	0·338847	0·642196
0·6	1·70422	0·402080	0·621873
0·7	1·74750	0·463098	0·597844
0·8	1·79675	0·521524	0·570058
0·9	1·85171	0·576990	0·538692
1·0	1·91204	0·629155	0·504136
1·1	1·97742	0·677729	0·466954
1·2	2·04746	0·722482	0·427854
1·3	2·12178	0·763262	0·387632
1·4	2·19998	0·799999	0·347127
1·5	2·28165	0·832706	0·307167
1·6	2·36639	0·861476	0·268520
1·7	2·45382	0·886476	0·231858
1·8	2·54356	0·907932	0·197723
1·9	2·63529	0·926118	0·166513
2·0	2·72869	0·941341	0·138480
2·1	2·82347	0·953924	0·113728
2·2	2·91940	0·964195	0·922376(−1)
2·3	3·01625	0·972476	0·738802(−1)
2·4	3·11384	0·979069	0·584466(−1)
2·5	3·21201	0·984254	0·456707(−1)
2·6	3·31065	0·988282	0·352536(−1)
2·7	3·40964	0·991373	0·268843(−1)
2·8	3·50890	0·993717	0·202566(−1)
2·9	3·60836	0·995473	0·150817(−1)
3·0	3·70798	0·996773	0·110967(−1)
3·1	3·80771	0·997724	0·806936(−2)
3·2	3·90751	0·998412	0·579994(−2)
3·3	4·00738	0·998903	0·412085(−2)
3·4	4·10729	0·999251	0·289444(−2)
3·5	4·20723	0·999494	0·200997(−2)
3·6	4·30719	0·999661	0·138005(−2)
3·7	4·40716	0·999776	0·936932(−3)
3·8	4·50714	0·999853	0·629012(−3)
3·9	4·60713	0·999905	0·417612(−3)
4·0	4·70712	0·999939	0·274203(−3)
4·1	4·80712	0·999961	0·178066(−3)
4·2	4·90711	0·999976	0·114372(−3)
4·3	5·00711	0·999985	0·726618(−4)
4·4	5·10711	0·999991	0·456625(−4)
4·5	5·20711	0·999994	0·283856(−4)
4·6	5·30711	0·999997	0·174556(−4)
4·7	5·40711	0·999998	0·106191(−4)
4·8	5·50711	0·999999	0·639102(−5)
4·9	5·60711	0·999999	0·380536(−5)
5·0	5·70711	1·00000	0·224166(−5)
5·1	5·80711	1·00000	0·130648(−5)
5·2	5·90711	1·00000	0·753376(−6)
5·3	6·00711	1·00000	0·429829(−6)
5·4	6·10711	1·00000	0·242664(−6)
5·5	6·20711	1·00000	0·135557(−6)
5·6	6·30711	1·00000	0·748920(−7)
5·7	6·40711	1·00000	0·409228(−7)
5·8	6·50711	1·00000	0·220994(−7)
5·9	6·60711	1·00000	0·117677(−7)
6·0	6·70711	1·00000	0·617579(−8)

those of H_{24} were slightly more than 0·1 per cent low. The values of the wall gradients f_0'' obtained from H_{12} and H_{24} were also low by somewhat less than 0·1 per cent.

Table 3(e). *Solution for* $\beta = -1, f_0 = (3)^{\frac{1}{2}}$

η	f	f'	f''
0·0	1·732050809	0·0000000	1·000000
0·1	1·73693	0·0965307	0·932333
0·2	1·75115	0·186743	0·872987
0·3	1·77409	0·271295	0·818696
0·4	1·80523	0·350572	0·767137
0·5	1·84404	0·424760	0·716725
0·6	1·89002	0·493922	0·666480
0·7	1·94266	0·558045	0·615911
0·8	2·00146	0·617090	0·564923
0·9	2·06590	0·671023	0·513732
1·0	2·13549	0·719844	0·462781
1·1	2·20970	0·763606	0·412657
1·2	2·28805	0·802425	0·364016
1·3	2·37003	0·836481	0·317516
1·4	2·45519	0·866020	0·273757
1·5	2·54309	0·891341	0·233239
1·6	2·63333	0·912788	0·196329
1·7	2·72553	0·930734	0·163253
1·8	2·81937	0·945569	0·134089
1·9	2·91456	0·957681	0·108785
2·0	3·01083	0·967449	0·871747(−1)
2·1	3·10798	0·975231	0·690032(−1)
2·2	3·20582	0·981354	0·539547(−1)
2·3	3·30421	0·986114	0·416775(−1)
2·4	3·40301	0·989770	0·318068(−1)
2·5	3·50213	0·992543	0·239841(−1)
2·6	3·60149	0·994623	0·178711(−1)
2·7	3·70104	0·996164	0·131596(−1)
2·8	3·80071	0·997293	0·957711(−2)
2·9	3·90049	0·998110	0·688921(−2)
3·0	4·00033	0·998694	0·489873(−2)
3·1	4·10022	0·999107	0·344358(−2)
3·2	4·20014	0·999396	0·239323(−2)
3·3	4·30009	0·999596	0·164451(−2)
3·4	4·40006	0·999732	0·111737(−2)
3·5	4·50004	0·999825	0·750745(−3)
3·6	4·60003	0·999886	0·498826(−3)
3·7	4·70002	0·999927	0·327786(−3)
3·8	4·80001	0·999954	0·213030(−3)
3·9	4·90001	0·999971	0·136936(−3)
4·0	5·00000	0·999982	0·870652(−4)
4·1	5·10000	0·999989	0·547569(−4)
4·2	5·20000	0·999993	0·340658(−4)
4·3	5·30000	0·999996	0·209653(−4)
4·4	5·40000	0·999998	0·127645(−4)
4·5	5·50000	0·999999	0·768854(−5)
4·6	5·60000	0·999999	0·458186(−5)
4·7	5·70000	1·00000	0·270162(−5)
4·8	5·80000	1·00000	0·157630(−5)
4·9	5·90000	1·00000	0·910170(−6)
5·0	6·00000	1·00000	0·520176(−6)
5·1	6·10000	1·00000	0·294357(−6)
5·2	6·20000	1·00000	0·165032(−6)
5·3	6·30000	1·00000	0·917210(−7)
5·4	6·40000	1·00000	0·506228(−7)

Table 3(f). *Solution for* $\beta = -1, f_0 = 2$

η	f	f'	f''
0·0	2·00000	0·000000	1·414213562
0·1	2·00678	0·132837	1·24764
0·2	2·02606	0·250385	1·10692
0·3	2·05642	0·354829	0·984535
0·4	2·09664	0·447735	0·875475
0·5	2·14562	0·530258	0·776479
0·6	2·20238	0·603297	0·685526
0·7	2·26599	0·667592	0·601456
0·8	2·33563	0·723798	0·523692
0·9	2·41050	0·772533	0·452021
1·0	2·48990	0·814405	0·386424
1·1	2·57317	0·850023	0·326957
1·2	2·65972	0·880002	0·273655
1·3	2·74901	0·904958	0·226478
1·4	2·84056	0·925497	0·185280
1·5	2·93398	0·942205	0·149805
1·6	3·02890	0·955637	0·119690
1·7	3·12501	0·966307	0·944916(−1)
1·8	3·22208	0·974682	0·737091(−1)
1·9	3·31989	0·981178	0·568125(−1)
2·0	3·41827	0·986156	0·432690(−1)
2·1	3·51708	0·989926	0·325643(−1)
2·2	3·61622	0·992748	0·242196(−1)
2·3	3·71560	0·994834	0·178025(−1)
2·4	3·81517	0·996360	0·129337(−1)
2·5	3·91486	0·997462	0·928791(−2)
2·6	4·01465	0·998249	0·659334(−2)
2·7	4·11450	0·998805	0·462719(−2)
2·8	4·21441	0·999193	0·321058(−2)
2·9	4·31434	0·999461	0·220260(−2)
3·0	4·41429	0·999643	0·149417(−2)
3·1	4·51427	0·999767	0·100232(−2)
3·2	4·61425	0·999849	0·664930(−3)
3·3	4·71423	0·999903	0·436251(−3)
3·4	4·81423	0·999939	0·283080(−3)
3·5	4·91422	0·999961	0·181683(−3)
3·6	5·01422	0·999976	0·115338(−3)
3·7	5·11422	0·999985	0·724281(−4)
3·8	5·21422	0·999991	0·449918(−4)
3·9	5·31421	0·999995	0·276486(−4)
4·0	5·41421	0·999997	0·168093(−4)
4·1	5·51421	0·999998	0·101109(−4)
4·2	5·61421	0·999999	0·601766(−5)
4·3	5·71421	0·999999	0·354414(−5)
4·4	5·81421	1·00000	0·206588(−5)
4·5	5·91421	1·00000	0·119215(−5)
4·6	6·01421	1·00000	0·681340(−6)
4·7	6·11421	1·00000	0·385967(−6)
4·8	6·21421	1·00000	0·217023(−6)
4·9	6·31421	1·00000	0·121375(−6)
5·0	6·41421	1·00000	0·677429(−7)

In view of the accurate solutions for no mass transfer contained in Paper 7, it was felt that the remaining gap in the real domain should be filled with more accurate data than interpolated solutions.

Table 4 contains such values, the solutions for $\beta = 1$, 2 and ∞, taken from Paper 7, being included for completeness. Solutions were first obtained on a computer using the method described in section 5 and Appendix B. However, these were found to contain some error, which will be discussed below; this error is believed to be caused by using too coarse an integration interval. Means were found to eliminate a large part of it, and Table 4 contains corrected values of the functions.

The values of f_0'' in Table 4 are those obtained by trial and error on the computer. They are believed to be very accurate since each is the better of a pair, one on either side of the correct value and differing by only one unit in the last significant digit.

Table 3(g). *Solution for* $\beta = -1, f_0 = (5)^{\frac{1}{2}}$

η	f	f'	f''
0·0	2·236067978	0·000000	1·732050809
0·2	2·26725	0·296193	1·26051
0·4	2·34930	0·513207	0·926372
0·6	2·46867	0·672057	0·672963
0·8	2·61515	0·786140	0·476178
1·0	2·78082	0·865565	0·325069
1·2	2·95963	0·918761	0·212861
1·4	3·14706	0·952884	0·133269
1·6	3·33991	0·973800	0·796528(−1)
1·8	3·53600	0·986036	0·454247(−1)
2·0	3·73396	0·992868	0·247192(−1)
2·2	3·93294	0·996509	0·128407(−1)
2·4	4·13245	0·998363	0·637055(−2)
2·6	4·33222	0·999264	0·302013(−2)
2·8	4·53212	0·999683	0·136886(−2)
3·0	4·73208	0·999869	0·593436(−3)
3·2	4·93206	0·999948	0·246182(−3)
3·4	5·13205	0·999980	0·977635(−4)
3·6	5·33205	0·999993	0·371795(−4)
3·8	5·53205	0·999997	0·135471(−4)
4·0	5·73205	0·999999	0·473319(−5)
4·2	5·93205	1·00000	0·158868(−5)
4·4	6·13205	1·00000	0·514836(−6)
4·6	6·33205	1·00000	0·163486(−6)
4·8	6·53205	1·00000	0·529870(−7)
5·0	6·73205	1·00000	0·193739(−7)
5·2	6·93205	1·00000	0·931421(−8)
5·4	7·13205	1·00000	0·617331(−8)
5·6	7·33205	1·00000	0·489061(−8)
5·8	7·53205	1·00000	0·421223(−8)
6·0	7·73205	1·00000	0·395722(−8)

Table 3(h). *Solution for* $\beta = -1, f_0 = (10)^{\frac{1}{2}}$

η	f	f'	f''
0·0	3·162277660	0·000000	2·828427126
0·2	3·20970	0·434615	1·63345
0·4	3·32409	0·686573	0·946194
0·6	3·47725	0·831423	0·537362
0·8	3·65245	0·912546	0·295398
1·0	3·83980	0·956377	0·156123
1·2	4·03361	0·979112	0·790724(−1)
1·4	4·23070	0·990405	0·383244(−1)
1·6	4·42938	0·995773	0·177680(−1)
1·8	4·62881	0·998214	0·788010(−2)
2·0	4·82858	0·999276	0·334397(−2)
2·2	5·02848	0·999719	0·135820(−2)
2·4	5·22845	0·999895	0·528184(−3)
2·6	5·42843	0·999962	0·196738(−3)
2·8	5·62843	0·999987	0·702252(−4)
3·0	5·82843	0·999996	0·240440(−4)
3·2	6·02843	0·999999	0·791418(−5)
3·4	6·22843	0·999999	0·252024(−5)
3·6	6·42843	1·00000	0·791200(−6)
3·8	6·62843	1·00000	0·258411(−6)
4·0	6·82843	1·00000	0·993131(−7)
4·2	7·02843	1·00000	0·520742(−7)
4·4	7·22843	1·00000	0·370644(−7)
4·6	7·42843	1·00000	0·311436(−7)
4·8	7·62843	1·00000	0·279267(−7)
5·0	7·82843	1·00000	0·255180(−7)
5·2	8·02843	1·00000	0·233798(−7)
5·4	8·22843	1·00000	0·215687(−7)
5·6	8·42843	1·00000	0·200711(−7)
5·8	8·62843	1·00000	0·186922(−7)
6·0	8·82843	1·00000	0·173875(−7)

Using the values of f' given by the computer, the boundary-layer thicknesses δ_1^* and δ_2^* and the other functions occurring in Table 4 were calculated. Because the solutions are not very satisfactory, the distributions of the stream function and its gradients are not given in the present paper.

The function E_2 is a correction to a linear approximation for the relationship between F_2 and λ_2 and is defined by the equation:

$$F_2 = 0{\cdot}44105 - 5{\cdot}1604\,\lambda_2 - E_2. \quad (101)$$

When the values of E_2 obtained from the computer solutions were plotted against $1/\beta$, some

Table 4. Solutions to the velocity equation for the real domain; $f_0 = 0$, β large

β	f_0''	δ_1^*	δ_2^*	H_{12}	H_{24}	$\lambda_2 \equiv \frac{\delta_2^2}{\nu}\frac{du_G}{dx}$	$F_2 \equiv \frac{u_G}{\nu}\frac{d\delta_2^2}{dx}$	E_2
1	1·2325877	0·64789	0·29235	2·2161	0·36035	0·085469	0·0	0·0
2	1·6872182	0·49741	0·23080	2·1552	0·38941	0·10654	−0·10654	−0·00220
3	2·043922	0·41902	0·19671	2·1301	0·40207	0·11609	−0·15479	−0·00323
4	2·347284	0·36893	0·17431	2·1165	0·40916	0·12154	−0·18230	−0·00382
5	2·615776	0·33336	0·15816	2·1077	0·41371	0·12507	−0·20012	−0·00426
7	3·083505	0·28514	0·13594	2·0975	0·41918	0·12937	−0·22177	−0·00476
10	3·675215	0·24076	0·11523	2·0893	0·42351	0·13279	−0·23902	−0·00517
20	5·180604	0·17212	0·082768	2·0796	0·42879	0·13701	−0·26032	−0·00566
∞	1·1547005	0·7785391	0·3761614	2·069694	0·4343538	0·1414974	−0·2829948	−0·00614

Notes: (1) Solutions for $\beta = 1, 2, \infty$ taken from the literature.
(2) The similar co-ordinates for $\beta = \infty$ are different from those for the other values.

scatter of the points was evident. The points for $\beta = 1, 2, \infty$ and -4 were on a smooth curve, those for $\beta = 3, 4$ and 5 were only slightly displaced from it and those for $\beta = 7, 10$ and 20 were a considerable distance away. The solution for $\beta = -4$, it will be realized, lies in the imaginary domain and was given by Mangler [7] (see also Table 1 in Paper 2).

The values of E_2 were therefore adjusted by drawing the most acceptable smoothed curve on this figure and reading off more accurate values. By means of these and the accurate values of f_0'', the other functions were recalculated. They differ from the values first obtained by less than one unit in the fourth significant digit. The error still remaining in most of the functions is believed to be less than three units in the last digit quoted.

9. INTERPOLATED SOLUTIONS FOR INFINITE β

9.1 *General Discussion*

Among the similar solutions given in Paper 2, a set corresponding to infinite β played an important rôle in the interpolation method employed. These were solutions to equation (27) with boundary conditions (28) and were obtained from calculations by Holstein [14]. In carrying out the interpolations, asymptotic values of thickness ratios for high blowing rates as given by Pretsch [4] were used. Since Paper 2 was written it has been found that these asymptotic values contain an appreciable error. It has already been seen in section 4 that the values are now known exactly.

It has also been possible to treat in the same way solutions to the other case of infinite β, namely equation (31) with boundary conditions (32), again using calculations by Holstein [14].

The opportunity has therefore been taken to re-examine these solutions and to draw up a new set of interpolated values of boundary-layer functions. These cover a much wider range of mass-transfer rate than the solutions given in Paper 2.

9.2 *Solutions by Holstein*

Holstein [14] gave solutions to equation (27), with boundary conditions (28), and equation (31), with boundary conditions (32), in the form of tables of the velocity $d\theta/d\xi$ (or $d\bar{\theta}/d\bar{\xi}$) and shear stress $d^2\theta/d\xi^2$ (or $d^2\bar{\theta}/d\bar{\xi}^2$) at intervals in the independent variable ξ (or $\bar{\xi}$). In some cases the values were at regular intervals in the independent variable ξ, in others at regular intervals in the velocity $d\theta/d\xi$. Solutions were given for a number of values of the mass-transfer parameter k_0. The stream function θ does not occur in the differential equation and was therefore not evaluated by Holstein.

In order to obtain the information required in the present work, it was necessary by numerical integration of Holstein's values to calculate one of the "similar" boundary-layer thicknesses δ_1^* or δ_2^*, which are now defined in

terms of the similar length co-ordinate ξ. When the interval in ξ was regular, a straightforward application of Simpson's rule to values of $[1 - (\mathrm{d}\theta/\mathrm{d}\xi)]$ supplied the thickness δ_1^*. When the interval was regular in $\mathrm{d}\theta/\mathrm{d}\xi$, and therefore irregular in ξ, the integration procedure was modified in the following manner.

(a) *When the variables are real*

In this case, equation (27) applies and the main-stream velocity distribution is that which occurs along the walls of a straight-walled, converging channel. It is convenient here to use primes to denote differentiation with respect to the similar distance co-ordinate ξ defined in equation (8). In terms of this co-ordinate, the displacement thickness δ_1^* is defined as:

$$\delta_1^* = \int_0^\infty (1 - \theta')\,\mathrm{d}\xi. \tag{102}$$

Since $\mathrm{d}\theta'/\mathrm{d}\xi = \theta''$, the integration variable in this can be changed from ξ to θ' to give:

$$\delta_1^* = \int_0^1 \frac{(1 - \theta')}{\theta''}\,\mathrm{d}\theta'. \tag{103}$$

This form is suitable for integrating Holstein's solutions at regular intervals in θ', except that the value of the integrand in the main-stream was not given. In its present form this is indeterminate, but let it be denoted by L. On differentiation of the numerator and the denominator and substitution for (θ'''/θ'') from the differential equation, it is found that:

$$L = \lim_{\xi\to\infty} \frac{(1 - \theta')}{\theta''} = \lim_{\xi\to\infty} -\frac{\theta''}{\theta'''}$$

$$= \lim_{\xi\to\infty} \frac{1}{k_0 + (1 - \theta')(1 + \theta')/\theta''}. \tag{104}$$

Since L now also occurs on the right it must satisfy the equation:

$$L = \frac{1}{k_0 + 2L} \tag{105}$$

and so has the value:

$$L = \frac{-k_0 \pm (k_0^2 + 8)^{1/2}}{4}. \tag{106}$$

The positive sign preceding the square root is appropriate for Holstein's solutions.

(b) *When the variables are pure imaginary*

In this case, equation (31) applies and the main-stream velocity distribution is that found along the walls of a straight-walled, diverging channel. Proceeding in the same way as above, if the value of $(1 - \bar{\theta}')/\bar{\theta}''$ in the main-stream is denoted by L_1 it is found to satisfy:

$$L_1 = \frac{1}{-\bar{k}_0 - 2L_1} \tag{107}$$

and therefore to have the value:

$$L_1 = \frac{-\bar{k}_0 \pm (\bar{k}_0^2 - 8)^{1/2}}{4} \tag{108}$$

where again the positive sign applies.

This method of integrating the functions given by Holstein is believed to be quite accurate since the integrand, when plotted as a function of θ', is only slightly curved and its values at the two ends of the range of integration are known accurately. By plotting in this way some scatter was in fact observed with some of Holstein's values near the main-stream. By using a large scale and drawing a smooth curve through the most acceptable points, however, this error was largely eliminated.

Values of the functions obtained from Holstein's solutions are given in Table 5. In the first five solutions the quantities k_0 and θ_0'' should be denoted by "barred" quantities since they refer to solutions to equation (31).

If the values of the thickness ratios H_{12} and H_{24} in Table 5 are examined, their variation with the mass-transfer parameter k_0 is not very satisfactory for large values of $|k_0|$ or $|\bar{k}_0|$. This is believed to be due to error in the original solutions probably brought about by the fact that the boundary layer is very thin and the integration interval too large.

It should be noted that no solutions to equation (31) which behave like real boundary layers exist for values of $|\bar{k}_0|$ less than $8^{1/2}$. The wall shear $\bar{\theta}_0''$ is still quite large for this mass-transfer rate so it is not because the boundary layer is about to "separate". What it does mean is that only with this minimum amount of suction can a boundary layer be maintained along the walls of a diverging channel, otherwise the boundary condition in the main-stream is contravened.

Table 5. Solutions for infinite β

k_0 (or $\bar{k}_0$)	θ_0'' (or $\bar{\theta}_0''$)	H_{12}	H_{24}	$\frac{v_0\delta_2}{\nu}$	$F_2\left(\equiv \frac{u_G}{\nu}\frac{d\delta_2^2}{dx}\right)$
$-8\frac{1}{3}$	1·9257	1·8888	0·6018	− 0·8839	0·1953
− 4	3·5694	1·989	0·5143	− 0·5763	0·04152
− 6	5·7372	1·986	0·5048	− 0·5280	0·01549
− 8	7·8070	2·018	0·4992	− 0·5115	0·008178
−10	9·8472	1·992	0·5029	− 0·5107	0·005213
10	10·1474	2·030	0·4950	− 0·4878	− 0·004746
4	4·3408	2·014	0·4905	− 0·4520	− 0·02555
2	2·5644	2·022	0·4789	− 0·3735	− 0·06974
− 2	0·4638	2·163	0·3612	1·558	− 1·213
− 4	0·2482	2·218	0·3276	5·279	− 3·484
−10	0·1000	2·202	0·3106	31·06	− 19·59

Functions evaluated from solutions given by Holstein [14]. Those in the first five lines apply to equation (31), the remainder to equation (27).

Table 6. Interpolated solutions for infinite β

$\frac{v_0\delta_2}{\nu}$	H_{12}	H_{24}	k_0 (or $\bar{k}_0$)	θ_0'' (or $\bar{\theta}_0''$)	$\lambda_2 \equiv \frac{\delta_2^2}{\nu}\frac{du_G}{dx}$
−0·8839	1·8888	0·6018	2·828	1·926	−0·09765
−0·85	1·9011	0·5885	2·831	1·960	−0·09014
−0·80	1·9198	0·5710	2·856	2·039	−0·07843
−0·75	1·9369	0·5556	2·915	2·159	−0·06619
−0·70	1·9520	0·5420	3·026	2·343	−0·05352
−0·65	1·9658	0·5300	3·226	2·630	−0·04046
−0·60	1·9786	0·5190	3·641	3·149	−0·02716
−0·55	1·9892	0·5085	4·677	4·324	−0·01382
−0·54	1·991	0·5065	5·104	4·787	−0·01120
−0·53	1·993	0·5048	5·778	5·501	−0·00842
−0·52	1·996	0·5032	6·945	6·721	−0·00561
−0·51	1·998	0·5016	9·635	9·477	−0·00280
−0·50	2·000	0·5000	∞	∞	0·0
−0·49	2·002	0·4980	9·492	9·647	0·00266
−0·48	2·004	0·4960	6·577	6·796	0·00533
−0·47	2·006	0·4940	5·260	5·529	0·00798
−0·46	2·007	0·4923	4·440	4·752	0·01074
−0·45	2·009	0·4905	3·879	4·228	0·01346
−0·40	2·018	0·4824	2·421	2·920	0·02730
−0·35	2·026	0·4750	1·722	2·338	0·04131
−0·30	2·034	0·4680	1·275	1·989	0·05537
−0·25	2·042	0·4614	0·9483	1·750	0·06949
−0·20	2·048	0·4551	0·6913	1·573	0·08369
−0·15	2·054	0·4492	0·4792	1·435	0·09797
−0·10	2·059	0·4439	0·2982	1·324	0·11242
−0·05	2·064	0·4389	0·1403	1·232	0·1269

Table 6.—continued

$\frac{v_0\delta_2}{\nu}$	H_{12}	H_{24}	k_0 (or $\bar{k}_0$)	θ_0'' (or $\bar{\theta}_0''$)	$\lambda_2 = \frac{\delta_2^2}{\nu}\frac{du_G}{dx}$
0·0	2·06969	0·434354	0·0	1·15470	0·141497
0·1	2·078	0·4261	−0·2419	1·031	0·1709
0·2	2·087	0·4192	−0·4466	0·936	0·2006
0·3	2·094	0·4130	−0·6249	0·8603	0·2305
0·4	2·101	0·4068	−0·7842	0·7975	0·2602
0·5	2·108	0·4010	−0·9286	0·7448	0·2899
0·6	2·114	0·3960	−1·609	0·7002	0·3198
0·7	2·120	0·3909	−1·184	0·6611	0·3496
0·8	2·126	0·3864	−1·299	0·6272	0·3795
0·9	2·131	0·3822	−1·406	0·5972	0·4095
1·0	2·137	0·3783	−1·509	0·5707	0·4394
1·2	2·147	0·3715	−1·698	0·5257	0·4994
1·4	2·156	0·3654	−1·872	0·4886	0·5594
1·6	2·165	0·3603	−2·033	0·4578	0·6194
1·8	2·172	0·3559	−2·183	0·4317	0·6797
2·0	2·178	0·3522	−2·325	0·4094	0·7402
2·2	2·183	0·3491	−2·458	0·3901	0·8009
2·4	2·187	0·3464	−2·585	0·3732	0·8618
2·6	2·191	0·3440	−2·707	0·3581	0·9226
2·8	2·195	0·3419	−2·824	0·3448	0·9834
3·0	2·198	0·3400	−2·936	0·3327	1·0444
3·5	2·204	0·3361	−3·199	0·3072	1·197
4·0	2·209	0·3330	−3·442	0·2866	1·350
4·5	2·213	0·3305	−3·670	0·2696	1·503
5·0	2·216	0·3285	−3·884	0·2552	1·657
6	2·221	0·3252	−4·282	0·2321	1·964
7	2·225	0·3227	−4·646	0·2142	2·271
8	2·229	0·3208	−4·984	0·1998	2·577
9	2·233	0·3193	−5·301	0·1881	2·883
10	2·235	0·3182	−5·599	0·1782	3·190
20	2·246	0·3126	−7·995	0·1250	6·258
∞	2·25889	0·306853	∞	0·0	∞

Solutions in the range $-0{\cdot}8839 \leqslant v_0\delta_2/\nu \leqslant -0{\cdot}5$ apply to equation (31) for which column 4 gives $\bar{k}_0$ and column 5 gives $\bar{\theta}_0''$; those in the range $-0{\cdot}5 \leqslant v_0\delta_2/\nu \leqslant \infty$ apply to equation (27) for which column 4 gives k_0 and column 5 gives θ_0''.

Referring to equation (108), this means that the function L_1 is real only when $|\bar{k}_0| \geqslant 8^{1/2}$.

9.3 *Interpolation*

The solutions contained in Table 5 are quite suitable for interpolation since, in addition to those quoted, the following three solutions for infinite β are also known exactly: (i) the case of infinite suction, (ii) the case $k_0 = 0$ in equation (27) (see Paper 7) and (iii) the case of infinite blowing treated in section 4.4.

With the quantity $(v_0\delta_2/\nu)$ as variable, or its reciprocal when considering intensive blowing, interpolated values of the thickness ratios H_{12} and H_{24} were therefore obtained and other functions calculated from them. The results are given in Table 6, where the function F_2 is not given since it is simply $-2\lambda_2$.

The accuracy of the values in this table is about the same as the interpolated solutions given in Paper 2; the values of the thickness ratios should be better than $\pm 0{\cdot}3$ per cent everywhere. Where any quantities in this table differ from those given in Paper 2, the present values are to be preferred.

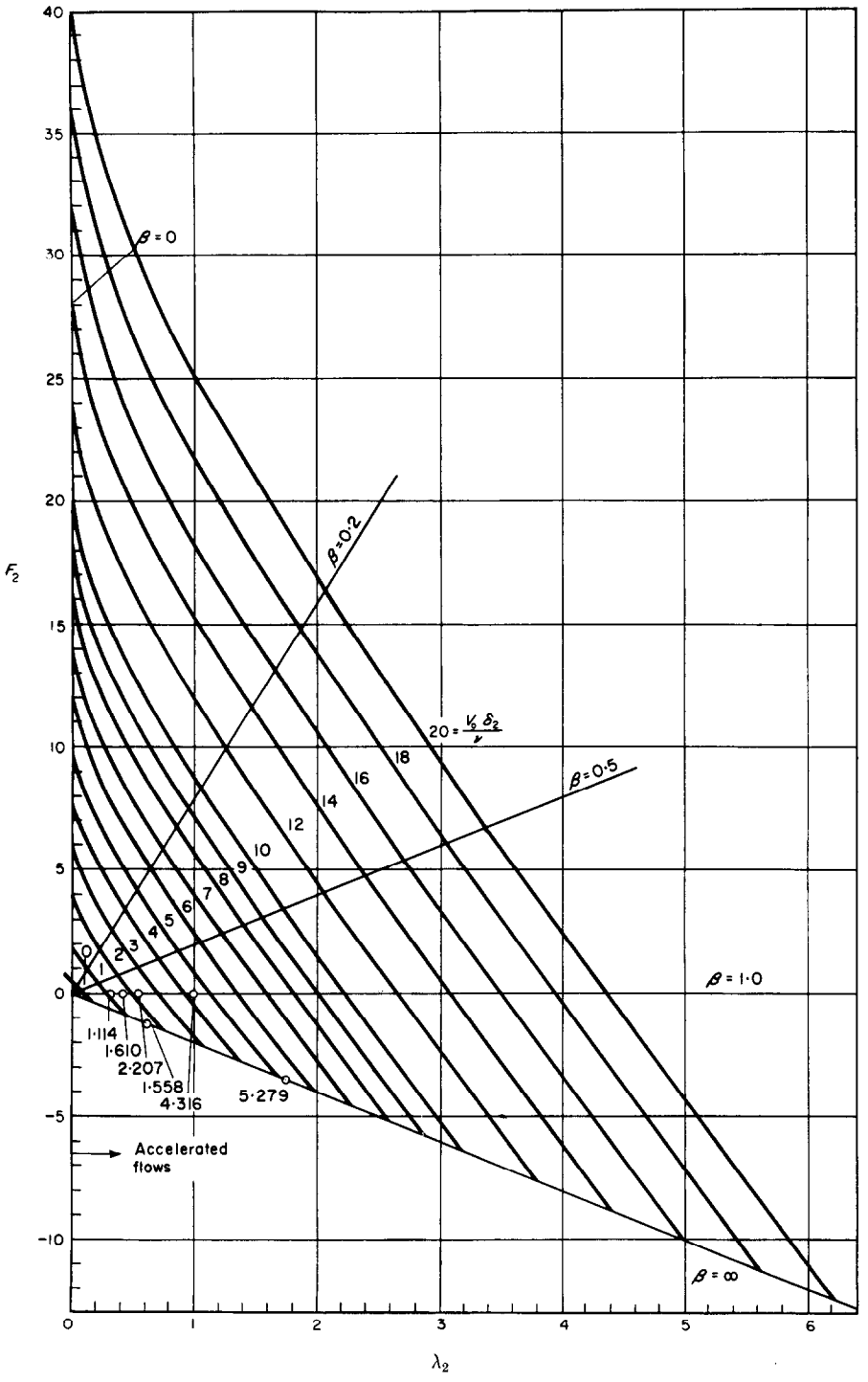

FIG. 2. Intensive blowing: F_2 as a function of λ_2 with $v_0\delta_2/\nu$ as mass-transfer parameter.

T

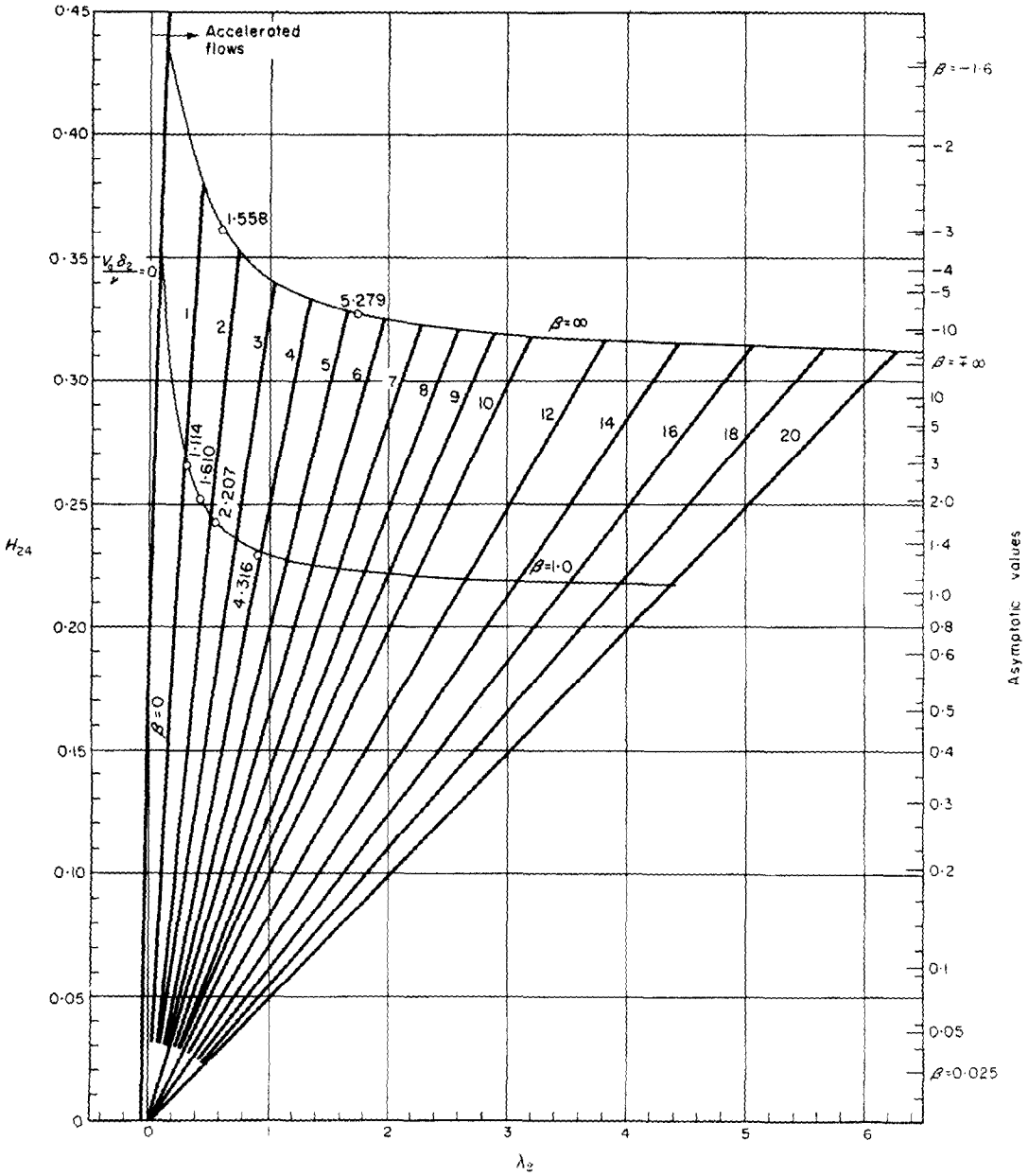

FIG. 3. Intensive blowing: H_{24} as a function of λ_2 with $v_0\delta_2/\nu$ as mass-transfer parameter.

10. VARIATION OF F_2 AND H_{24} WITH λ_2 FOR INTENSIVE BLOWING

In the method of boundary-layer analysis contained in Papers 1 and 2, curves were required showing the variation with the pressure-gradient parameter λ_2 of the growth function F_2 and the thickness ratio H_{24}. The highest blowing rate included in the interpolated solutions of Paper 2 was for $(v_0\delta_2/\nu) = 3{\cdot}0$. By means of the method to be explained below, these curves are extended to $(v_0\delta_2/\nu) = 20{\cdot}0$ with the results shown in Figs. 2 and 3.

The shapes of the curves showing the variation of F_2 were first obtained by assuming that the thickness ratios H_{12} and H_{24} had the asymptotic values for high blowing rates given in Table 1. These curves cut the vertical axis, where the pressure gradient is zero, at the exact value, since it is known that, when the blowing rate is large enough, $F_2 = 2(v_0\delta_2/\nu)$ along that line. For any other pressure gradient, however, these preliminary curves were displaced from the correct position.

By interpolation along the lines $\beta = 1{\cdot}0$ and $\beta = \infty$, their positions were obtained more accurately in this region. While retaining the same general shape the preliminary curves were then displaced so as to pass through the interpolated points. In the final form of the curves given in Fig. 2, the accuracy is believed to be such that the position of any point is correct to within ± 3 per cent of its distance from the origin.

Very few exact solutions to the equations occur in this region and most of them are shown in Fig. 2 with values of the parameter $(v_0\delta_2/\nu)$ nearby.

Curves for H_{24} shown in Fig. 3 were easier to draw, since, on this scale, the origin and interpolated points for $\beta = 1{\cdot}0$ and $\beta = \infty$ were in the same straight line for almost all the values of $(v_0\delta_2/\nu)$ covered. The solution for $(v_0\delta_2/\nu) = 4{\cdot}316$, obtained by Schlichting and Bussman [6], is seen to be slightly displaced from the line $\beta = 1{\cdot}0$ in Fig. 3. In view of the great difficulty of obtaining exact solutions in this region it is not surprising that this solution contains some error.*

* *Note added in proof:* A large number of solutions, like those for $\beta = 1$ given in the present paper, have now been computed. They cover a wide range of positive and negative β with f_0 in the range $0 \leqslant f_0 \leqslant 3{\cdot}0$. The equations for infinite β have also been integrated accurately for wide ranges in the mass transfer parameter. Finally, the suggestion made in the introduction that asymptotic expansions for infinite blowing may give good accuracy, has been found to work well, at least for obtaining values of f_0''!

ACKNOWLEDGEMENTS

The work reported in the present paper is part of the research programme of the Division of Food Preservation, C.S.I.R.O., Australia. The author wishes to express his gratitude to the staff of the Adolph Basser Computing Laboratory, University of Sydney where many of the numerical solutions were obtained, and to Miss J. D. Hayhurst who carried out most of the other calculations and helped to prepare the work for publication. He is also grateful for most constructive criticism from a referee which enabled the original text to be improved in a number of places.

REFERENCES

1. D. B. SPALDING, Mass transfer through laminar boundary layers—1. The velocity boundary layer. *Int. J. Heat Mass Transfer*, **2**, 15–32 (1961). Referred to as Paper 1.
2. D. B. SPALDING and H. L. EVANS, Mass transfer through laminar boundary layers—2. Auxiliary functions for the velocity boundary layer. *Int. J. Heat Mass Transfer*, **2**, 199–221 (1961). Referred to as Paper 2.
3. H. L. EVANS, Mass transfer through laminar boundary layers—7. Further similar solutions to the b-equation for the case $B = 0$. *Int. J. Heat Mass Transfer*, **5**, 35–57 (1962). Referred to as Paper 7.
4. J. PRETSCH, Die laminare Grenzschicht bei starkem Absaugen und Ausblasen. *Dtsch. Luftf.* U.M. 3091 (1944).
5. E. J. WATSON, The asymptotic theory of boundary layer flow with suction. *Brit. Aero. Res. Council R. and M.* 2619 (1952).
6. H. SCHLICHTING and K. BUSSMAN, Exakte Lösungen für die laminare Reibungsschicht mit Absaugung und Ausblasen. *Schr. dtsch. Akad. Luftf.* **7B**, Nr. 2, 25 (1943).
7. W. MANGLER, Boundary layers—1·2 Special exact solutions, *AVA Monogr. Rep. and Transl.* No. 1001 (Ed. W. TOLLMIEN) (1948).
8. A. M. O. SMITH, Improved solutions of the Falkner and Skan boundary layer equations. *Rep. E.S.* 16009 (Contract No. NOa(s) 9027) Douglas Aircraft Co. Inc. (1952).
9. R. M. TERRILL, Laminary boundary-layer flow near separation with and without suction. *Phil. Trans. Roy. Soc.* A **253**, No. 1022, 55 (1960).
10. E. R. G. ECKERT, P. L. DONOUGHE and B. J. MOORE, Velocity and friction characteristics of laminar viscous boundary layer and channel flow with ejection or suction. *N.A.C.A.* TN 4102 (1957).
11. B. THWAITES, The development of the laminar boundary layer under conditions of continuous suction—I. On similar profiles. *A.R.C. Rep.* 11,830 (1948).

12. B. THWAITES, The development of laminar boundary layers under conditions of continuous suction—II. Approximate methods of solution. *A.R.C. Rep.* 12,699 (1949).
13. B. THWAITES, On two solutions of the boundary layer equations, in 50 *Jahre Grenzschichtforschung* (Ed. H. GOERTLER and W. TOLLMIEN), 210 (1955).
14. H. HOLSTEIN, Ähnliche laminare Reibungschichten an durchlässigen Wänden. *Dtsch. Luftf.* U.M. 3050 (1943).
15. S. GILL, A method for the step-by-step integration of differential equations in an automatic digital computing machine. *Proc. Camb. Phil. Soc.* **47**, 96 (1951).

APPENDIX A

Boundary-layer Functions for High Rates of Mass Transfer

The results obtained in section 4 are summarized below.

(a) *Intensive suction*

From equation (50) of the text, the stream function f has the form:

$$f = f_0 + \eta - \frac{1}{f_0}(1 - e^{-f_0\eta}). \tag{A1}$$

The velocity distribution in the boundary layer is:

$$\frac{u}{u_G} = (1 - e^{-f_0\eta}) \tag{A2}$$

and the wall gradient is:

$$f_0'' = f_0. \tag{A3}$$

The other boundary-layer functions have the following values:

$$\left.\begin{aligned} -\frac{v_0\delta_2}{\nu} = H_{24} = \tfrac{1}{2}, \quad H_{14} = 1, \\ H_{12} = 2, \quad F_2 = \lambda_2 = 0. \end{aligned}\right\} \tag{A4}$$

(b) *Intensive blowing when β is not infinite*

From equation (76) of the text the velocity distribution is:

$$\frac{u}{u_G} = \left\{1 - \left(\frac{f}{f_0}\right)^{2\beta}\right\}^{1/2} \tag{A5}$$

and the dimensionless wall shear is:

$$f_0'' = -\frac{\beta}{f_0}. \tag{A6}$$

The thickness ratio H_{24} has the value:

$$H_{24} = \beta - \frac{\pi^{1/2}}{4}\frac{\Gamma(1/2\beta)}{\Gamma[\frac{3}{2} + (1/2\beta)]} \tag{A7}$$

and the other ratios are obtained from this by means of:

$$H_{12} = \frac{1}{H_{24}} - \left(1 + \frac{1}{\beta}\right) \tag{A8}$$

and

$$H_{14} = 1 - \left(1 + \frac{1}{\beta}\right) H_{24}. \tag{A9}$$

The ratio H_{24} is related to the pressure gradient parameter λ_2 by:

$$H_{24} = \frac{\nu}{v_0\delta_2}\lambda_2. \tag{A10}$$

Numerical values of these thickness ratios are given in Table 1.

(c) *Intensive blowing when β is infinite*

The stream function has the form:

$$\theta = -k_0 \ln\left(\cosh - \frac{\xi}{k_0}\right) \tag{A11}$$

and the velocity distribution is:

$$\frac{u}{u_G} = \tanh\left(-\frac{\xi}{k_0}\right). \tag{A12}$$

The thickness ratios have the following values:

$$H_{24} = (1 - \ln 2), \; H_{14} = \ln 2, \; H_{12} = \frac{\ln 2}{(1 - \ln 2)}. \tag{A13}$$

APPENDIX B

Solving Equation (18) on a Computer

With the following definitions:

$$p = f \tag{B1}$$

$$q = f' \tag{B2}$$

$$r = f'' \tag{B3}$$

equation (18) is reduced to the following set of simultaneous first-order differential equations:

$$\frac{d\eta}{d\eta} = 1 \tag{B4}$$

$$\frac{dp}{d\eta} = q \tag{B5}$$

$$\frac{dq}{d\eta} = r \tag{B6}$$

$$\frac{dr}{d\eta} = -pr - \beta(1 - q^2). \tag{B7}$$

It should be noted that the quantity $s = \int_0^n f\,d\eta$, which is important in evaluating solutions to the b-equation (see earlier papers in the present series) can also be evaluated. Since its gradient with respect to η is f, this merely means adding the equation $ds/d\eta = p$ to this set.

Although equation (B4) appears to be trivial, the method to be described requires it. Equations (B4–7) apply to the real domain; to work in the imaginary domain the only change required is to alter the sign of the right-hand side of equation (B7).

The initial conditions are:

$$\eta_0 = 0 \tag{B8}$$

$$p_0 = f_0 \tag{B9}$$

$$q_0 = 0 \tag{B10}$$

$$r_0 = f_0''. \tag{B11}$$

The set of equations (B4–7) is now solved numerically at regular intervals in the variable η by means of the following Runge–Kutta process developed by Gill [15]. Each of the four equations is of the form:

$$\frac{dw_i}{d\eta} = h_i\,(w_1, w_2, w_3, w_4) \tag{B12}$$

where w_i is one of the variables η, p, q or r, and the function h_i, written in (B12) as a function of the variables w_i, represents the right-hand side of the relevant equation.

Let the magnitude of the interval in η be ϵ. The values of the variables w at the beginning of an interval being known, the value of any one of them, say w_i, at the end of the interval is obtained by a routine consisting of four stages. The stages all have the same form but each employs a different set of numerical coefficients. Using a second suffix j to denote a particular stage, at each stage the following functions are evaluated:

$$s_{i,\,j} = \epsilon h_i(w_{1,\,j}, w_{2,\,j}, w_{3,\,j}, w_{4,\,j}) \tag{B13}$$

$$m_{i,\,j+1} = A_j\,s_{i,\,j} - B_j\,t_{i,\,j} \tag{B14}$$

$$w_{i,\,j+1} = w_{i,\,j} + m_{i,\,j+1} \tag{B15}$$

$$t_{i,\,j+1} = t_{i,\,j} + 3m_{i,\,j+1} - C_j\,s_{i,\,j} \tag{B16}$$

in which the numerical coefficients A_j, B_j and C_j take the following values for the four stages:

j	A_j	B_j	C_j
0	1/2	1	1/2
1	$(1 - 1/\sqrt{2})$	$(1 - 1/\sqrt{2})$	$(1 - 1/\sqrt{2})$
2	$(1 + 1/\sqrt{2})$	$(1 + 1/\sqrt{2})$	$(1 + 1/\sqrt{2})$
3	1/6	1/3	1/2

At the end of each fourth stage ($j = 3$) the quantities $t_{i,\,4}$ and $w_{i,\,4}$ obtained from equations (B15) and (B16) are retained and used at the beginning of the next interval. The quantities $m_{i,\,j+1}$ are used only within a particular stage and so are not retained. The quantity $w_{i,\,4}$ is, of course, the new value of the function w_i.

The operations within each interval are carried out in the following order:

$$\begin{aligned} j &= 0 \quad i = 1, 2, 3, 4 \\ j &= 1 \quad i = 1, 2, 3, 4 \\ j &= 2 \quad i = 1, 2, 3, 4 \\ j &= 3 \quad i = 1, 2, 3, 4. \end{aligned}$$

APPENDIX C

Gradients of the Stream Function

In boundary-layer theory it is often useful to obtain expansions of the stream function, or one of its derivatives, about some point either within the boundary layer or at its extremities. Expansions about the wall have, for example, been used in several of the earlier papers in the present series.

To obtain such expansions, many derivatives of the stream function are required. Knowing the

value of the stream function and its first two derivatives, the third derivative is obtained simply by substituting these into the differential equation, namely the first expression in the list given below. Derivatives of higher order are then obtained by substituting the lower-order derivatives into expressions obtained by successive differentiation of the differential equation.

The expressions for evaluating derivatives up to f^{XV} for similar solutions are given below. In these the negative signs on the left-hand sides should be used for the real domain and the positive signs for the imaginary domain. In the nomenclature of the present paper these quantities should be denoted by "barred" quantities when working in the imaginary domain.

$$\mp f''' = ff'' + \beta(1 - f'^2)$$

$$\mp f^{IV} = ff''' + (1 - 2\beta) f' f''$$

$$\mp f^{V} = ff^{IV} + (2 - 2\beta) f' f''' + (1 - 2\beta) (f'')^2$$

$$\mp f^{VI} = ff^{V} + (3 - 2\beta) f' f^{IV} + (4 - 6\beta) f'' f'''$$

$$\mp f^{VII} = ff^{VI} + (4 - 2\beta) f' f^{V} + (7 - 8\beta) f'' f^{IV} + (4 - 6\beta) (f''')^2$$

$$\mp f^{VIII} = ff^{VII} + (5 - 2\beta) f' f^{VI} + (11 - 10\beta) f'' f^{V} + (15 - 20\beta) f''' f^{IV}$$

$$\mp f^{IX} = ff^{VIII} + (6 - 2\beta) f' f^{VII} + (16 - 12\beta) f'' f^{VI} + (26 - 30\beta) f''' f^{V} + (15 - 20\beta) (f^{IV})^2$$

$$\mp f^{X} = ff^{IX} + (7 - 2\beta) f' f^{VIII} + (22 - 14\beta) f'' f^{VII} + (42 - 42\beta) f''' f^{VI} + (56 - 70\beta) f^{IV} f^{V}$$

$$\mp f^{XI} = ff^{X} + (8 - 2\beta) f' f^{IX} + (29 - 16\beta) f'' f^{VIII} + (64 - 56\beta) f''' f^{VII} + (98 - 112\beta) f^{IV} f^{VI} + (56 - 70\beta) (f^{V})^2$$

$$\mp f^{XII} = ff^{XI} + (9 - 2\beta) f' f^{X} + (37 - 18\beta) f'' f^{IX} + (93 - 72\beta) f''' f^{VIII} + (162 - 168\beta) f^{IV} f^{VII} + (210 - 252\beta) f^{V} f^{VI}$$

$$\mp f^{XIII} = ff^{XII} + (10 - 2\beta) f' f^{XI} + (46 - 20\beta) f'' f^{X} + (130 - 90\beta) f''' f^{IX} + (255 - 240\beta) f^{IV} f^{VIII} + (372 - 420\beta) f^{V} f^{VII} + (210 - 252\beta) (f^{VI})^2$$

$$\mp f^{XIV} = ff^{XIII} + (11 - 2\beta) f' f^{XII} + (56 - 22\beta) f'' f^{XI} + (176 - 110\beta) f''' f^{X} + (385 - 330\beta) f^{IV} f^{IX} + (627 - 660\beta) f^{V} f^{VIII} + (792 - 924\beta) f^{VI} f^{VII}$$

$$\mp f^{XV} = ff^{XIV} + (12 - 2\beta) f' f^{XIII} + (67 - 24\beta) f'' f^{XII} + (232 - 132\beta) f''' f^{XI} + (561 - 440\beta) f^{IV} f^{X} + (1012 - 990\beta) f^{V} f^{IX} + (1419 - 1584\beta) f^{VI} f^{VIII} + (792 - 924\beta) (f^{VII})^2.$$

Zusammenfassung—Es werden Probleme der hydrodynamischen Grenzschicht behandelt, für den Fall einheitlicher Stoffwerte und Stofftransport in beliebiger Richtung durch die wandnahe Schicht. Zur Nachprüfung des asymptotischen Verhaltens der Grenzschichtfunktionen bei grossem Stoffdurchsatz dient die "ähnliche" Form der Geschwindigkeitsgleichung. Die Verhältnisse der Grenzschichtdicken bei intensiver Anblasung H_{14}, H_{12} und H_{24} sind tabelliert.

Die in der Rechenmaschine verwendete Integrationsmethode ist beschrieben und folgende numerische Lösungen sind angegeben: (1) Exakte Lösungen für $\beta = 1$, den vorderen Staupunkt der zweidimensionalen Strömung, wobei der Stoffübergang-Parameter f_0 dreizehn verschiedene Werte $-3{,}0 \leqslant f_0 \leqslant 3{,}0$ annahm. (2) Exakte Lösungen für $\beta = -1$ im reellen Bereich, bei acht Werten von f_0 von $\sqrt{2}$ am Trennpunkt, bis $\sqrt{10}$ bei asymptotischer Annäherung an das Unterdruckgebiet. (3) Lösungen von etwas geringerer Genauigkeit für den reellen Bereich ohne Stofftransport, bei grossen β-Werten. (4) Interpolationslösungen für unendliche Werte von β mit Stofftransport; dabei sind sowohl reelle wie imaginäre Werte der Variablen berücksichtigt.

Um die Abhängigkeit von F_2, des Anwachsens der Geschwindigkeitsgrenzschicht, vom Druckgradienten, und die Änderung des Dickenverhältnisses H_{24} für einen Bereich des Stoffdurchsatzes von $0 \leqslant (v_0\delta_2/\nu) \leqslant 20{,}0$ zu zeigen, sind Kurven angegeben. Ein Anhang bringt Formeln zur Auswertung höherer Ableitungen der Stromfunktion.

Аннотация—Рассматривается задача о динамическом пограничном слое с постоянными физическими параметрами среды при подаче (поглощении) вещества через стенку обтекаемого тела. «Подобные» решения уравнения движения используются для получения асимптотических выражений ранее полученных вспомогательных функций (условных толщин пограничного слоя) при больших плотностях поперечного потока вещества. Даны таблицы величин H_{14}, H_{12} и H_{24} для значительных интенсивностей подаваемого через стенку вещества.

Описан метод интегрирования уравнения на счётно-решающем приборе и даны следующие численные решения:

(1) Точные решения для $\beta = 1$ (передняя критическая точка двухмерного потока) и $f_0 = -3{,}0\ (0{,}5)\ 3{,}0$ (всего тринадцать значений);

(2) Точные решения для $\beta = -1$ и восьми значений f_0 от $\sqrt{2}$ в точке отрыва до величины $\sqrt{10}$, соответствующей асимптотическому отсасыванию;

(3) Несколько уступающие предыдущим по точности решения в действительной области при отсутствии массообмена и больших значениях β;

(4) Интерполированные решения при $\beta = \infty$ и наличии массообмена. В эту совокупность входят как действительные, так и мнимые значения переменных.

Даны графики кривых, которые показывают изменение функции F_2, характеризующей темп нарастания пограничного слоя, и толщины H_{24} при различных градиентах давления, когда интенсивность массообмена дежит в пределах $0 \leqslant (v_0\delta_2/\nu) \leqslant 20{,}0$. В приложении даются формулы для расчёта производных более высоких порядков от функции тока.